

PHYSICO-CHEMICAL AND KINETIC STUDIES OF  
A NICOTINAMIDE ADENINE DINUCLEOTIDE SPECIFIC  
GLUTAMIC DEHYDROGENASE FROM BLASTOCLADIELLA EMERSONII

by

Susan G. Jackson



A Thesis  
Submitted to  
the Faculty of Graduate Studies and Research  
In Partial Fulfilment  
of the Requirements for the Degree  
Master of Science

1969

c Susan G. Jackson 1969

TO MY PARENTS

The writer wishes to thank Dr. H.B. LeJohn  
for his patient and generous assistance.

## ABSTRACT

An NAD-specific glutamic dehydrogenase was isolated from the mitochondria of Blastocladiella emersonii and some of its kinetic properties were studied. Various purine nucleotides participated as positive (ADP, AMP) or negative (ATP, GTP, GDP) allosteric effectors. The nucleotide effect showed a strong correlation with the pH of the assay system. In the oxidative deamination of glutamate AMP (or ADP), at saturating levels, converted complex non-linear double reciprocal plots into Michaelian-type plots. For the reductive amination of  $\alpha$ -ketoglutarate the shape of the double reciprocal (rate-concentration) plots was unchanged with saturating levels of AMP. These plots were normally linear with a sharp threshold level caused by substrate inhibition.

On the basis of product inhibition studies an Ordered Binary-Ternary kinetic mechanism (Cleland, W.W., Biochem. Biophys. Acta, 67, 104, 1963) was proposed for the oxidative deamination reaction.

Zone sedimentation analysis by sucrose density gradients revealed that protons, effectors, and some substrates protected the enzyme against hydrodynamic inacti-

vation. At alkaline pH (pH 9) the enzyme is inactivated by sedimentation. Inclusion of  $\text{NAD}^+$ ,  $\text{NADH}$ ,  $\text{AMP}$ ,  $\text{Ca}^{++}$ , and to a lesser extent, glutamate and  $\alpha$ -ketoglutarate stabilized the enzyme against inactivation. At pH 6, the enzyme remained partially active after sedimentation but, of all substrates,  $\text{NAD}^+$  was peculiar in that it caused a complete inactivation of the enzyme. All other substrates and effectors failed to appreciably enhance recovery at pH 6 but did not cause inactivation.

LéJohn (Biochem. Biophys. Res. Commun., 32, 278, 1968) has been able to show a pH dependence on the regulatory action of  $\text{Ca}^{++}$  and  $\text{Mn}^{++}$  on the enzyme. Both cations inhibit the oxidative deamination reaction unidirectionally and activate the reductive amination of  $\alpha$ -ketoglutarate. An extension of these studies led to evidence of unidirectional inhibition of the oxidative deamination reaction by the metabolites citrate, isocitrate, fumarate, succinate, fructose 1, 6-diphosphate and the non-metabolite EDTA (LéJohn, H.B., J. Biol. Chem., 243, 5126, 1968). Among the metabolites, citrate was the strongest inhibitor. This inhibition could be relieved by various cations and AMP.

From these studies a molecular model of the enzyme action has been proposed. Also a generalized physiological

concept involving the regulation of this enzyme and a "linked" mitochondrial NAD-specific isocitric dehydrogenase (McCrea, B.E., M.Sc. Thesis, Univ. of Manitoba, 1969) has been formulated.

## ABBREVIATIONS

ADP	adenosine diphosphate
AMP	adenosine 5' monophosphate
ATP	adenosine triphosphate
CDP	cytosine diphosphate
CTP	cytosine triphosphate
DEAE-cellulose	diethylaminoethyl-cellulose
EDTA	(sodium) ethylenediamine tetra acetic acid
GDP	guanosine diphosphate
GTP	guanosine triphosphate
IDH	isocitric dehydrogenase
IMP	inosine monophosphate
ITP	inosine triphosphate
NAD <sup>+</sup>	nicotinamide adenine dinucleotide (oxidized)
NADH	nicotinamide adenine dinucleotide (reduced)

## TABLE OF CONTENTS

	<u>Page</u>
INTRODUCTION -----	1
HISTORICAL	
I. Organism -----	3
II. Allosteric Models -----	5
III. Adenylate Control Hypothesis -----	12
IV. Glutamic Dehydrogenase -----	14
MATERIALS AND METHODS	
I. Growth Conditions -----	17
II. Extraction Procedure -----	18
III. Assay System -----	19
IV. Kinetics -----	20
V. Sucrose Density Gradients -----	20
VI. Mitochondrial Preparation -----	22
VII. Chemicals -----	23
RESULTS	
I. A) Rate-concentration patterns with and without modifiers -----	24
B) Determination of Michaelis constants with and without AMP -----	34
II. A) Product Inhibition Studies -----	44
B) A Kinetic Mechanism -----	53
III. pH Effect on Kinetics -----	58
IV. Interactions of pH and Purine Nucleotides -----	60

## RESULTS - Cont'd.

V. Zone Sedimentation Analysis by Sucrose Density Gradients -----	63
VI. Influence of Cations on Substrate-substrate Interactions -----	68
VII. Dependence of Cationic Effects on pH -----	74
VIII. Mitochondrial Work -----	76
IX. Unidirectional Inhibition by Metabolites -----	76
DISCUSSION	
Section A. A Molecular Mechanism -----	82
Section B. A Physiological Model of Mitochondrial Regulation -----	90
I. Physiological Regulation of Glutamic Dehydrogenase -----	90
II. Generalized Pattern of Mitochondrial Regulation -----	96
REFERENCES -----	100

## LIST OF FIGURES

<u>Figure</u>		<u>Page</u>
1.	Rate of the oxidative deamination of glutamate catalysed by <u>Blastocladiella</u> glutamic dehydrogenase as a function of (a) $\text{NAD}^+$ levels and (b) glutamate concentration.	25
2.	Rate of the oxidative deamination of glutamate as a function of $\text{NAD}^+$ concentration with expanded scale to emphasize the nature of the saturation curve at low substrate levels.	26
3.	Rate of the reductive amination of $\alpha$ -ketoglutarate catalysed by <u>Blastocladiella</u> glutamic dehydrogenase as a function of (o) $\text{NH}_4^+$ and (●) $\alpha$ -ketoglutarate concentrations. AMP added as indicated.	27
4.	Interactions between $\text{NAD}^+$ and glutamate at several levels of AMP for the oxidative deamination of glutamate.	30
5.	Interactions between $\text{NAD}^+$ and glutamate at several levels of ATP.	32

<u>Figure</u>	<u>Page</u>
6. "Binding-type" curves of the interactions between AMP and ATP at fixed levels of glutamate and $\text{NAD}^+$ (AMP the variable substrate).	35
7. Double reciprocal plots of rate of the oxidative deamination of glutamate against $\text{NAD}^+$ concentration.	37
8. Double reciprocal plots of rate of the oxidative deamination of glutamate against glutamate concentration.	39
9. Double reciprocal plots of rate of reductive amination of $\alpha$ -ketoglutarate against NADH concentration.	41
10. Double reciprocal plots of the rate of the oxidative deamination of glutamate against $\text{NAD}^+$ concentration.	42
11. Double reciprocal plots of rate of the reductive amination of $\alpha$ -ketoglutarate against NADH concentration in the presence of AMP.	45

<u>Figure</u>	<u>Page</u>
12. Product inhibition by NADH. Double reciprocal plots of rate of the oxidative deamination of glutamate against $\text{NAD}^+$ concentration.	47
13. Product inhibition by $\text{NH}_4^+$ . Double reciprocal plots of rate against $\text{NAD}^+$ concentration.	48
14. Product inhibition by $\text{NH}_4^+$ . Double reciprocal plots of rate against $\text{NAD}^+$ concentration. Glutamate saturating.	49
15. Product inhibition by $\text{NH}_4^+$ . Double reciprocal plots of rate against glutamate concentration.	50
16. Product inhibition by $\alpha$ -ketoglutarate. Double reciprocal plots of rate against $\text{NAD}^+$ concentration.	51
17. Product inhibition by $\alpha$ -ketoglutarate. Double reciprocal plots of rate against glutamate concentration.	52

<u>Figure</u>	<u>Page</u>
18. The effect of pH on the rate of the oxidative deamination of glutamate.	59
19. Interactions between pH and AMP at fixed concentrations of $\alpha$ -ketoglutarate, NADH and $\text{NH}_4^+$ .	61
20. Interactions between pH and AMP at fixed high concentrations of $\text{NAD}^+$ and glutamate.	62
21. Zone sedimentation analysis of <u>Blastocladiella</u> glutamic dehydrogenase in sucrose density gradients. Gradients contained 250-300 $\mu\text{g}$ enzyme protein with or without effectors and pH as indicated.	65
22. Rate-concentration representation of the effect of $\text{Ca}^{++}$ on the oxidative deamination of glutamate.	71
23. Lineweaver-Burk representation of the effect of $\text{Ca}^{++}$ , AMP, and ATP on the reductive amination of $\alpha$ -ketoglutarate with $\alpha$ -ketoglutarate as the variable substrate.	72

<u>Figure</u>		<u>Page</u>
24.	Double reciprocal plot of rate of the reductive amination of $\alpha$ -ketoglutarate against NADH concentration with and without $\text{Ca}^{++}$ and AMP.	73
25.	An allosteric model for <u>Blastocladiella</u> glutamic dehydrogenase.	83
26.	A Physiological Model of Mitochondrial Regulation.	92
27.	Rate of $\text{NAD}^+$ reduction catalyzed by an NAD-specific isocitric dehydrogenase from <u>Blastocladiella</u> at different citrate levels against $\text{NAD}^+$ concentration.	98

## INTRODUCTION

Recently much work has been done on "allosteric regulation" of key enzymes in cell metabolism. The enzymes of the citric acid cycle and those at its branch points have received particular attention because of their central importance in aerobic metabolism. The nature of cellular differentiation may be looked upon as discrete problems of biochemical equilibria under genetic control. Because of the ease and rapidity of growth, and the fact that it is a unicellular organism which displays several of the differentiating characteristics attributed to multicellular organisms, Blastocladiella emersonii provides a near ideal system for studies of cellular differentiation. Alteration of environmental factors such as light, chemical composition of the growth medium, and temperature, can lead to a change from an ordinary colourless (O.C.) actively growing cell to a resistant sporangial (R.S.) form (by Cantino's designation, see review (5)). Because one can easily identify different morphological forms during the ontogeny of the organism, it is possible to correlate form and function, at least superficially, in this fungus. In the past two decades a large body of disconnected

evidence has accumulated on the physiological characteristics of the organism. No attempt has been made to study the nature of regulation of enzymes, hitherto suspected to be involved, directly or indirectly, with the change in ontogeny induced by agents such as light, bicarbonate, and temperature (see review of Cantino and Lovett, (5) for an excellent account.) An NADP-specific isocitric dehydrogenase and isocitritase have been implicated in a physiological scheme of reversal of the citric acid cycle and CO<sub>2</sub> fixation by  $\alpha$ -ketoglutarate dehydrogenase. It has also been inferred from labelling studies, that labelled glutamate easily entered the citric acid cycle intermediates but labelled glucose entered glutamate with great difficulty (4). The purpose of this investigation was: (i) to identify and isolate the enzyme(s) responsible for glutamate synthesis and catabolism via organic acid intermediates; (ii) to study its mode of regulation, if any; and (iii) to correlate these findings with known physiological effects of the influence of diverse cations, glutamate, and citrate on the growth of the organism. The interest in cationic effects derives from the natural habitat of the fungus. Being a freshwater aquatic organism, one can easily appreciate the importance of inorganic ions in the overall development of the mould.

## HISTORICAL

I. Organism

Blastocladiella emersonii is a non-filamentous ('unicellular') water mould. The normal life cycle briefly is as follows. Motile zoospores retract their single flagellum and send out a germ tube which is destined to become the rhizoidal system of the plant. Exponential growth ensues for a period of 16 to 18 hours at 20°C. During this period, several nuclear divisions take place within each zoosporangium. The size of the sporangium increases several hundred-fold. At the termination of growth a septum delineates a sterile, subterminal rhizoidal cell which is virtually devoid of cytoplasm. The multinucleate terminal cell differentiates to form unimitochondrial zoospores which are subsequently discharged through papillae. This description represents the life cycle of the ordinary colourless (O.C.) plant (5). Variation of light, temperature, or growth medium constituents, however, can lead to an alternate form - the resistant sporangial (R.S.) form. The R.S. form builds up a thick wall and such cell constituents as soluble polysaccharide, carotenoids, melanin, chitin and it delays its zoospore release. The R.S. form has a life cycle of about 72 hours. Addition of exogenous bicarbonate

to the medium is one method of inducing this form. There exists a "point of no return" (at 36 hours) before which the R.S. form may revert to the O.C. form (e.g., by removal of bicarbonate). Beyond this point, however, the cell is irrevocably committed to the R.S. form. Thus, despite the lack of sexual reproduction this organism provides a near ideal system for studies in cell differentiation specifically with regard to enzymological study of regulation by known physiological effectors. Of particular interest is the effect of various substances on zoospore germination (LéJohn, unpublished data). Germination is inhibited by  $\text{Ca}^{++}$ , EDTA, and citrate. On the other hand, certain ions -  $\text{Mn}^{++}$ ,  $\text{Mg}^{++}$ , and  $\text{K}^+$  enhance germination. Also, although zoospores are actively respiring, there is no evidence for nucleic acid or protein synthesis within the spores.

Enzymological studies have indicated differential rates of synthesis of certain cell constituents during exponential growth (5). An example of this phenomenon is the case of glucose-6-phosphate dehydrogenase (17). The total amount of this enzyme increases exponentially. Between 30 and 60 per cent of the generation time this rate is greater than the exponential rate of synthesis of soluble protein and is identical to that for increase in dry weight per cell. On the contrary, the total activity

of isocitritase per cell is diluted during exponential growth until about one-half generation time (40).

Labelling studies (4) indicated that glutamate could easily enter citric acid cycle intermediates but that the carbons of glucose entered glutamate with difficulty. This observation, although perhaps not convincingly substantiated, led to interest in glutamic dehydrogenase as an important branch point enzyme of the citric acid cycle. The implication of substances involved in germination inhibition as effectors of glutamic dehydrogenase (LéJohn, unpublished data) provides interesting regulatory implications of glutamic dehydrogenase in the germination process.

## II. Allosteric Models

Regulation of enzymic catalysis by specific metabolites via conformational change was first proposed to explain feedback inhibition commonly found in many biosynthetic pathways (23, 42, 56). Atkinson (2) surveyed the literature and discussed how enzyme reactions may be controlled in a rather 'coarse' fashion through competitive inhibition between products and substrates. Monod, Changeux, and Jacob (42) initially proposed that direct steric hindrance between substrate and inhibitor may be impossible for stereochemically

unrelated molecules. This led to the concept that at least two stereo specifically different, non-overlapping but interacting sites are involved. The binding of the effector molecule induces a conformation change in the enzyme and this alters the binding property of the substrate site. A year earlier Gerhart and Pardee (16) had produced experimental evidence for this in their studies of aspartate transcarbamylase. Monod et al (42) coined the term allosterism to account for effectors which affect the substrate site through binding at a second (non-catalytic) site. Reiner (49) has pointed out that, if "acting at a second site" is meant, the term should be "allotropic". If on the other hand "shape changing" is meant the term should be "morphallactic" or "morphallaxic". Thus, he considers that the term allosteric, in itself, may be an improper connotation.

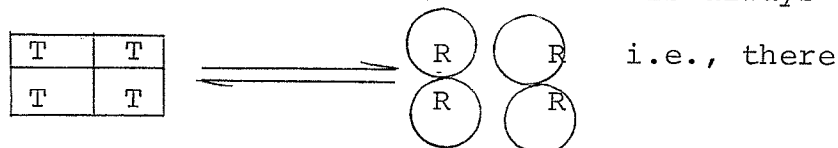
More recently Monod, Wyman, and Changeux (43) developed a statistical treatment of so-called "allosteric transitions" of regulatory enzymes. Their concept is based on the observation that the most important allosteric phenomena occur in oligomeric proteins including enzymes. A key element in the Monod-Wyman-Changeux formulation is that strict symmetry is maintained at all times during configurational changes of the enzyme. The model, outlined below, is subject to many refinements and

modifications. Most of the work reported in this thesis will provide ample evidence for one possible refinement of this theory.

The concept of Monod et al is that oligomeric proteins are regulated via homotropic and heterotropic effectors leading to cooperative and antagonistic effects. A homotropic effector is a ligand whose binding affects the binding and possibly the catalytic behaviour of other sites for the same ligand. Heterotropic effectors alter the properties of sites reacting with dissimilar ligands. Either of these could lead to cooperative effects (increasing binding and reaction rates of other sites) and antagonistic effects (decrease in binding and reaction rates). Such complex interactions may produce K systems (substrate itself is an allosteric ligand) where binding properties are affected. It must be realized that a change in  $K_m$  is not a definition for a K system since  $K_m$  is only a function of  $K_s$  (the actual binding constant). This system is distinguished from a V system in which the reaction rates are modified (substrate does not show cooperative interaction but effectors do).

Several other models based on statistical and kinetic premises have been formulated (3, 25, 50) but the model of Monod et al, is unique because of its symmetry restriction. This model shows a best fit to a homotropic cooperative

effect in a K system. As an example, the 'monomers' of a tetrameric enzyme are postulated to exist in two (at least) major conformational states designated R and T. These forms are in thermodynamic equilibrium with each other. The T form has a larger dissociation constant ( $K_t$ ) for a given ligand than R does (i.e.,  $K_t > K_r$ ). The assumption is that transition of the tetramer is always complete.



are no hybrids of the type:

T	T
T	R

 or
 

T	T
R	T

 or
 

R	R
R	R

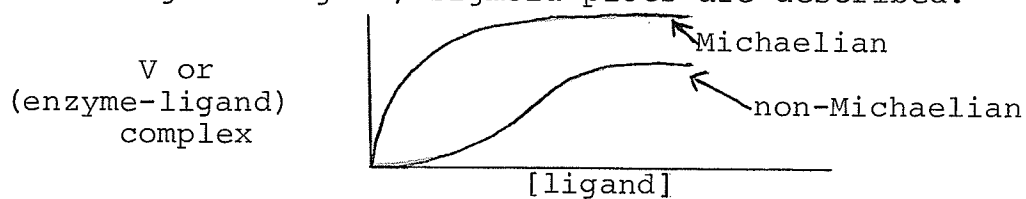
 or
 

T	T
R	R

 or
 

T	T
R	R

Thus, a given ligand stabilizes one configuration. Unless ligands are saturating, there would be, at any instant, a mixture of R and T forms. Hence, by titrating the enzyme with a given ligand, sigmoid plots are described.



The precise form of the titration plot will depend on the ratio of  $K_r$  to  $K_t$  and the value of  $L$  ("allosteric constant").

This relationship affords facility for an extension of the Monod-Wyman-Changeux concept as observed earlier. If, in addition to conformation changes, the enzyme can be subjected to aggregation and dissociation of catalytically active forms, then the simple sigmoid plot may become further

distorted into a mixture of hyperbolic and sigmoidal patterns (30). Such complex plots have been designated  $3/2$  and  $2/1$  functions by the algebraic kinetic analysts (6, 7, 51). The fractional functions denote the power of certain constants present in algebraic formulations of the probable number of catalytically active binding sites for different substrates. These descriptions, nevertheless, fail to elucidate the molecular nature of the protein even by detailed computer analyses.

Because great emphasis has been placed on the quaternary state of the Blastocladiella glutamic dehydrogenase in these studies, this aspect must be surveyed briefly. All quaternary forms of oligomeric proteins relate to association and dissociation of subunits. These subunits are not covalently bonded in the quaternary state. In this case monomer will be defined as that unit with one active site. Associated and dissociated forms of this refer to oligomer and subunit respectively. All protomers (subunits in an oligomer) occupy equivalent positions within the oligomer. The domain of bonding between any two protomers consists of two linked binding sets. (A binding set consists of a spatially organized collection of all protomeric groups which participate in binding to another.) Isologous associations are symmetrical and involve two identical binding sets. Consequently, there is a requirement for a finite structure with at least one axis of symmetry. Thus,

dimers and tetramers only are possible. Heterologous associations lack symmetry and can lead to greater than two protomers in association. A mixture of the two types leads to an even-numbered oligomer with a minimum of six protomers.

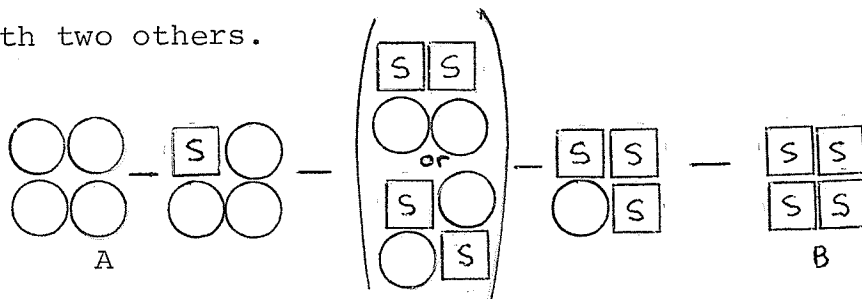
The conformation of each protomer can be constrained by its associations leading to the form T. Upon relaxation of constraints each protomer tends toward an alternate conformation (R). In such a transition the molecular symmetry, including protomeric constraints, is conserved.

Considering the extreme cases of dissociation and association, the symmetry of protomers may be destroyed upon the formation of 'super' aggregates or monomers irrespectively. The possibility exists that quaternary constraints may not induce a conformational change but only a (symmetrical) redistribution of electronic charges within the protein.

This model was based largely on studies of haemoglobin. The dissociation curve of oxyhaemoglobin as a function of oxygen tension is sigmoid showing a cooperative effect on binding sites. Haemoglobin is subject to the Bohr effect. That is, an increase of oxygen dissociation occurs as the pH is lowered. Wyman (58) showed that the Bohr effect is due to a discharge of protons provoked by the binding of oxygen.

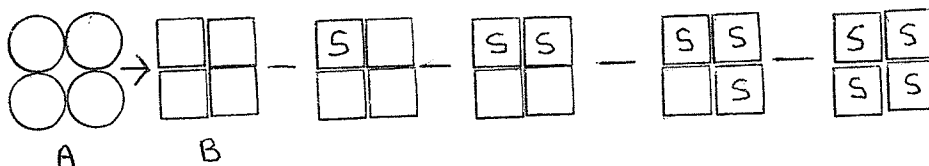
An extension of the regulatory significance of subunit interaction is contained in the molecular models of Koshland, Némethy, and Filmer (25). For simplicity identical subunits were considered primarily although this is not an essential precept.

The theory of Koshland et al considered two conformations, A and B, with the latter able to bind substrate (S). In the "square" model illustrated below diagonal interactions are considered negligible and thus each subunit interacts with two others.



i.e., non-equivalence of subunit interaction in progressive substrate binding.

The "concerted" model, unlike the rest, does not require that form B be present only in the presence of S:



This model is theoretically similar to that of Monod et al (43). The chief distinction is that the M-W-C model is restrictive by its symmetry premise whereas the K-N-F model ignores symmetry.

Two mechanisms may be considered for conformation change: catalysed transformation in which S accelerates the rate of change, and tautomerism whereby the protein itself changes to the new state which is subsequently complexed by S. The proposed "square" model of Koshland et al fits closely the binding data obtained for haemoglobin.

Certain assumptions of this theory should be considered. First, only two conformations are present. Also strong interactions exist between adjacent B conformations (similar to "constrained" form of Monod et al). The third assumption, that A-A and A-B interactions are equivalent, seems weak. It seems implausible that a change inducing strong interaction between B forms would not alter A-B interactions. By extension of the model to include an intermediate form, this discrepancy could be resolved.

### III. Adenylate Control

Studies on phosphofructokinase from various sources had indicated stimulation by AMP (cyclic and non-cyclic) (45, 46). Hathaway and Atkinson (19) had found AMP to be a positive modifier (i.e., activator) for yeast NAD-specific isocitric dehydrogenase. AMP produced a marked decrease in the half-saturation  $(S)_{0.5}$  for isocitrate. Atkinson (2) proposed that for isocitric dehydrogenase,

assuming the aconitase reaction to be near equilibrium, the result of AMP action would be that the levels of isocitrate and citrate would vary in opposition to that of AMP.

Citrate was found to be a positive modifier of acetyl CoA carboxylase (57) which is the first enzyme unique to fatty acid synthesis. Therefore, Hathaway and Atkinson (19) proposed that one regulatory property of acetyl CoA carboxylase acting in concert with isocitric dehydrogenase is to ensure fatty acid synthesis when AMP is low and reverse this trend as the AMP level rises.

It has been suggested further that glycogen synthetase and phosphofructokinase similarly ensure polysaccharide formation when ATP is high and glycolysis as ATP drops.

From these studies an adenylate control theory was proposed. It predicted that AMP or ADP modulation would in general be found at metabolic branch points between biosynthetic and degradative pathways. On the basis of this proposal energy control of metabolism may be examined by studies on how the momentary AMP/ADP/ATP ratio affects each metabolic branch point between energy production or storage.

#### IV. Glutamic dehydrogenase

Glutamic dehydrogenase occupies an important position at a branch point between organic acid and amino acid metabolism. Extensive study has been carried out with this enzyme mainly from animal tissues (10-14, 53, 55). The discovery of a reversible aggregation-disaggregation reaction of the bovine liver enzyme as a function of protein concentration (44) led to intensive investigation of this phenomenon. Dilution produces disaggregation. Frieden (11) found that relatively high concentrations of NADH led to dissociation of the enzyme polymer (molecular weight  $1 \times 10^6$ ) into monomers (molecular weight 350,000). These monomers could be further dissociated into subunits of molecular weight about 50,000. Tompkins et al (55), however, found no disaggregation with NADH alone but argued that  $ZnCl_2$ , GTP, diethylstilbestrol (DES), and ATP in the presence of high NADH levels did cause a reduction in molecular weight. It was found that ADP and certain amino acids (leucine, isoleucine, and methionine) protected the enzyme from disaggregation and consequent inhibition of activity. Dissociation could also be produced by the aromatic chelator, o-phenanthroline.

Tompkins, Yielding, and Curran (54) found that conditions promoting disaggregation simultaneously stimulated alanine dehydrogenase activity and consequently proposed a disaggregation effect on substrate specificity. Other workers found no such relationship (9).

Recently Frieden and Colman (14) have done extensive studies on protein concentration as a determinant in aggregation-disaggregation reactions. By kinetic and binding studies it was determined that in the presence of coenzyme, GTP and GDP bind more tightly to the monomer while ADP binds preferentially to the polymer. Cooperativity in the former case is evident only at enzyme concentrations greater than 0.1 mg/ml. Further studies showed that in the absence of purine nucleotides the specific activity of the enzyme was essentially independent of enzyme concentration.

Frieden (10) had proposed that the monomer was the lowest molecular weight species to be catalytically active. He proposed that two sites, at least exist (12). The first site, the active site, could bind any of four coenzymes [NAD(H), NADP(H)]. The second site he called the purine nucleotide site. Some evidence was also found for a third site specific for NADH. The last two sites would be allosteric sites.

Frieden (12) had proposed a reversible equilibrium scheme as follows:  $P \rightleftharpoons X \rightleftharpoons Y$  where P is the polymer and X and Y are the active and inactive monomers respectively.

Initially it was believed that, although glutamic dehydrogenase from animal sources was responsive in varying degrees to purine nucleotides, the enzyme from microorganisms and plants showed little response to these effectors. Frieden (13) felt it was significant that the enzyme from lower and higher plants displayed specificity for one or the other coenzyme while the mammalian enzyme was nonspecific. He proposed that the purine nucleotide effect had importance in regulating the use of a particular coenzyme. Recent studies with microorganisms, however, would tend to refute this proposal. Two species of glutamic dehydrogenase, each specific for one coenzyme, have been found in certain microorganisms (27, 28, 29). In Blastocladiella emersonii a single, NAD-specific enzyme has been found (30). A definite purine nucleotide modulation has been shown for many cases (27, 29, 52). Specifically AMP activation seems a consistent property of several of the enzymes from microorganisms (27, 29, 30). An alternate reason for the existence of the two activities with distinctly different controls must be sought.

## MATERIALS AND METHODS

I. Growth Conditions

The 'unicellular' water mold Blastocladiella emersonii was routinely grown for enzyme extraction in ten litre synchronous cultures. Standard zoospore inocula were obtained by growth on peptone-yeast-glucose (PYG) agar (5). PYG agar consists of 1.25 g bacteriological peptone, 1.25 g yeast extract, 3.0 g glucose per litre with 2 per cent Bacto-agar) in Roux bottles for 16 hours at 24°C. Sporulation was induced in mature plants by addition of 10 to 20 ml 'sporulating solution' (S.S.) (Trizma-maleate buffer, pH 6.7,  $10^{-3}$  M;  $\text{CaCl}_2$   $10^{-3}$  M). Roux bottles were subsequently allowed to stand for 15 to 20 minutes. The resultant zoospore suspension was then collected in an Erlenmeyer flask by sterile filtration through a loosely-packed cotton plug in the neck of a funnel. The spore suspension thus obtained may be used as inoculum for large cultures. Ten to twelve Roux bottles provided sufficient inoculum for a ten litre culture.

Cells were regularly grown in 10 litres PYG broth with antifoam-A and potassium phosphate buffer, pH 7,  $10^{-3}$  M in twelve litre carboys. Carboys were autoclaved for 45 minutes at 15 psi and were forcibly aerated for two to

three days before inoculation. Cultures were allowed to grow with forced aeration for 16 hours at 24°C. The mature zoosporangial plants were collected by filtering with suction through No. 1 Whatman filter paper. The zoosporangial mat was then washed with 2 litres 0.005 M phosphate buffer, pH 7.0, and dried by suction for 5 minutes. Cells could then be frozen at -20°C until required.

## II. Extraction Procedure

Extracts were obtained from cells with a wet weight of approximately 40 g. Cells were suspended with the aid of mortar and pestle in one volume of 0.1 M Tris-acetate buffer, pH 6.5, containing  $10^{-4}$  M reduced glutathione (GSH). An equivalent weight of glass powder (sand-type) was added and the suspension macerated with mortar and pestle for about 5 min. The suspension was then transferred to a mini-mill (Gifford-Wood Co., N.Y., 115 v 1.4 amp 60 cycles, AC-DC, with an optimum speed of 22,000 r.p.m., Vernier setting at 112) and homogenized for 10-15 min with the container immersed in an ice-salt bath. The homogenate was filtered through Whatman No. 1 filter paper under suction. The glass powder and residue were washed with buffer. The crude extract was then centrifuged at 48,000 X g for 10 min. All operations from this point on

were conducted at 5°C.

The crude extract was adsorbed directly onto a column of washed DEAE-cellulose (30 x 2.5 cm) pre-equilibrated with 0.05 M Tris-acetate buffer, pH 6.5, containing GSH ( $10^{-4}$  M).

The enzyme was eluted from the column with a linear gradient of 0 to 1 M KCl in 0.05 M Tris-acetate; 0.01 M phosphate buffer, pH 7.0, containing  $10^{-4}$  M EDTA. Enzyme from pooled eluates was then precipitated with ammonium sulphate at 55-60 per cent saturation. The precipitate was allowed to form over two hours with constant stirring. The precipitate was then collected by centrifugation (48,000 X g for 20 min) and resuspended in a small volume of starting buffer with 0.1 M KCl. The suspension can be dialyzed against the starting buffer for 2 hrs and used as such or further purified.

This partly purified enzyme preparation was then adsorbed on to a G-200 Sephadex column (30 X 2.5 cm) and the enzyme eluted with the starting buffer used in DEAE-cellulose chromatography containing 0.1 M KCl. The purified enzyme could be stored at -20°C until required.

### III. Assay System

The enzyme activity was determined by the reductive amination assay procedure. The assay mixture contained

10 mM  $\alpha$ -ketoglutarate, 0.33 mM NADH, 0.5 M  $\text{NH}_4^+$ , 1 mM AMP in 150 mM Tris-chloride buffer, pH 7.0, in a total volume of 3 ml. A typical enzyme purification is shown in Table I.

#### IV. Kinetics

All kinetic studies were carried out with a Gilford Model 2000 multiple channel recording spectrophotometer using 3 ml silica cuvettes with 10 mm light path. Optical density changes at 340 m $\mu$  were recorded with unit enzyme activity expressed as a change of .001 O.D. units per minute. Protein concentrations were determined by the method of Lowry et al (36).

Reactions were carried out at pH 9 for the oxidative deamination of glutamate and at pH 7.0 for the reductive amination of  $\alpha$ -ketoglutarate unless otherwise specified. The reaction systems used in various kinetic studies are summarized in the figure legends accompanying such illustrations.

#### V. Sucrose Density Gradients

Sucrose gradients were prepared by the method of Martin and Ames (38). The 4% to 20% (W/V) sucrose gradients were prepared in a Buchler Densigrad apparatus (Buchler

Table I

Purification of Blastocladiella emersonii glutamic dehydrogenase

Assay System as given in text.

Step	Volume	Total Units	Total Protein	Specific Activity
Crude	80	320,000	3,520 mg	91
DEAE-cellulose column	145	368,400	406 mg	907
Ammonium Sulphate Precipitation	5.7	230,000	62.2 mg	3,673
Sephadex Column	12	168,400	9.6 mg	17,500

Purification = 192 fold

Instruments, Fort Lee, N.J., U.S.A.). Gradients contained 0.1 M Tris-chloride buffer at various pH values and effectors were added as specified in each experiment. Centrifugations were carried out with 5 ml. sucrose gradient solutions in an SW 39 rotor in a Spinco Model L ultracentrifuge for 20 hours at an average speed of 30,000 r.p.m. between 5° and 10°C. Ten drop fractions were collected with a Buchler piercing unit (Buchler Instruments Co., Fort Lee, N.J., U.S.A.) and 34 fractions were obtained for the gradient lying between the meniscus and the head of the piercing needle. A 0.25 ml volume of 20% sucrose acted as a cushion from the bottom of the tube to the head of the needle.

Molecular weight determination was conducted and calculation was done by substitution into the equation:

$$\left( \frac{S_1}{S_2} \right) = \left( \frac{MW_1}{MW_2} \right)^{2/3}$$

where  $S_1$  and  $S_2$  are the distances travelled from the meniscus by enzymes of unknown and known molecular weights respectively, and  $MW_1$  and  $MW_2$  are their respective molecular weights.

## VI. Preparation of Mitochondria

A suspension of zoospores of Blastocladiella emersonii was prepared as described (18) in "mitochondrial suspending"

medium (0.25 M sucrose,  $10^{-4}$  M EDTA, .05 M potassium phosphate buffer, pH 7). Zoospores were disrupted by rapid freezing and thawing. Suspension was then centrifuged at 10,000 x g for 15 min. The pellet was washed once by recentrifuging in the suspending buffer to remove contaminating supernatant solution. The pellet was disrupted in a small volume of 0.05 M Tris-acetate, 0.05 M potassium phosphate buffer, pH 7,  $10^{-4}$  M EDTA) by repeated trituration before assay for glutamic dehydrogenase activity. Assay was carried out by the method described previously.

#### VII. Chemicals

Chemicals used were of the highest purity available commercially.

## RESULTS

I. A. Rate-concentration patterns with and without modifiers

Rate-concentration curves were obtained for all substrates for both the oxidative deamination and reductive amination reactions of Blastocladiella emersonii NAD-specific glutamic dehydrogenase.

Curves obtained for the reduction of  $\text{NAD}^+$  are illustrated in Fig. 1. With  $\text{NAD}^+$  as the variable substrate and glutamate fixed at very high and very low concentrations (Fig. 1a) it is apparent that classical Michaelis-Menten hyperbolic plots are not obtained. Similarly, with glutamate as the variable substrate and  $\text{NAD}^+$  fixed at reasonably high and low levels, hyperbolic plots were not obtained (Fig. 1b). It must be emphasized that the shape of the curves obtained depends largely on the scale of the abscissa. With the compressed scales employed in Fig. 1 an 'apparent' cooperative interaction between  $\text{NAD}^+$  and glutamate is seen although this interaction is evident for glutamate only at low  $\text{NAD}^+$  concentrations (Fig. 1b). When the scale is expanded to cover the lowest possible substrate concentrations which yield a measureable rate, hyperbolic saturation plots are obtained (Fig. 2).

Saturation curves obtained for the reductive amination of  $\alpha$ -ketoglutarate are shown in Fig. 3. Evidently

Figure 1. Rate of the oxidative deamination of glutamate catalysed by Blastocladiella glutamic dehydrogenase as a function of (a)  $\text{NAD}^+$  concentration; glutamate levels as indicated; and (b) glutamate concentration;  $\text{NAD}^+$  levels as indicated. The reaction mixtures contained 0.2 M Tris-chloride buffer, pH 9; 22  $\mu\text{g}$  enzyme protein.

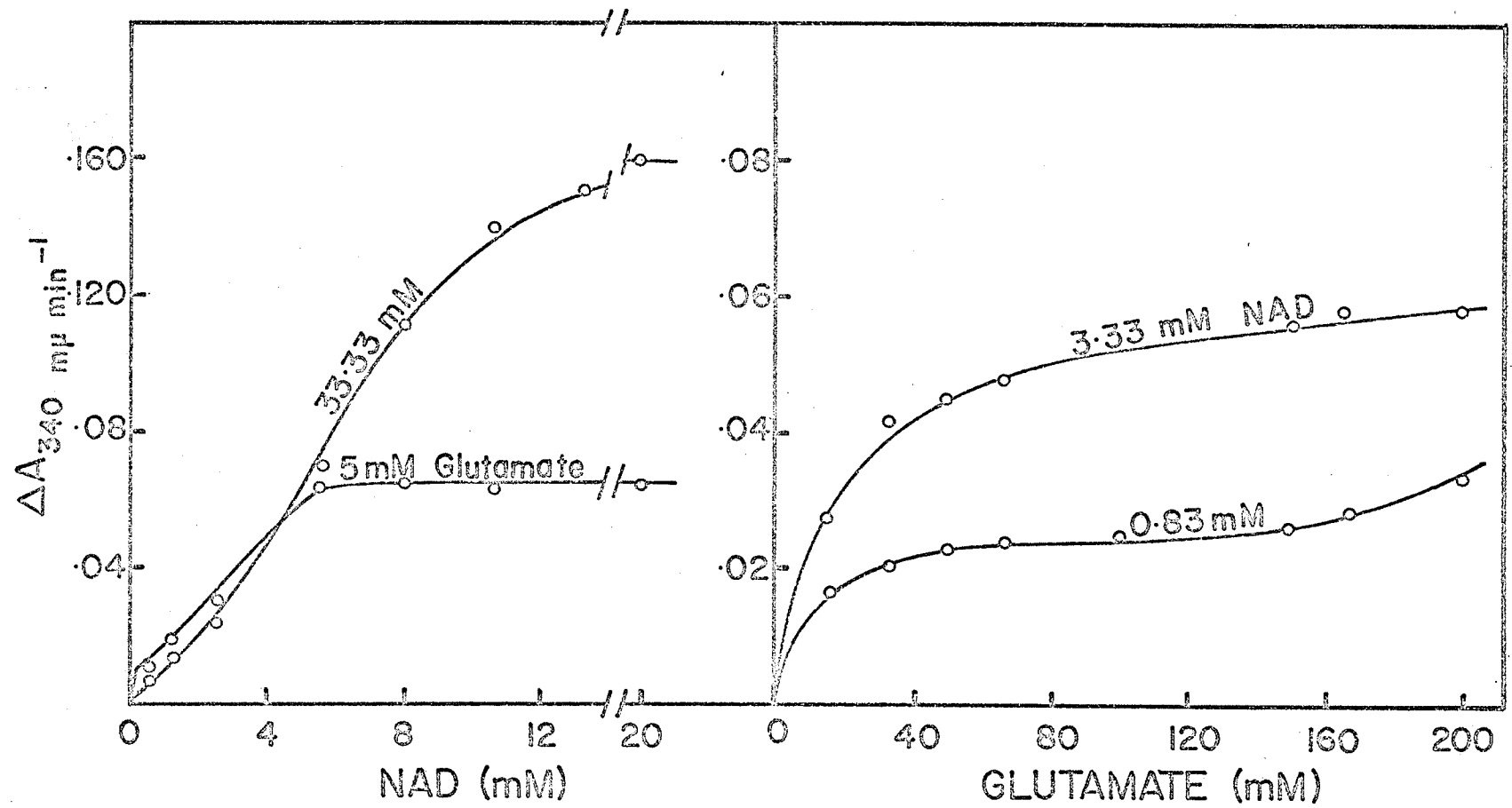


Figure 2. Rate of the oxidative deamination of glutamate as a function of  $\text{NAD}^+$  concentration with glutamate levels as indicated. The scale has been expanded to emphasize the nature of the saturation curve at low substrate levels. Reaction mixture as in Fig. 1a.

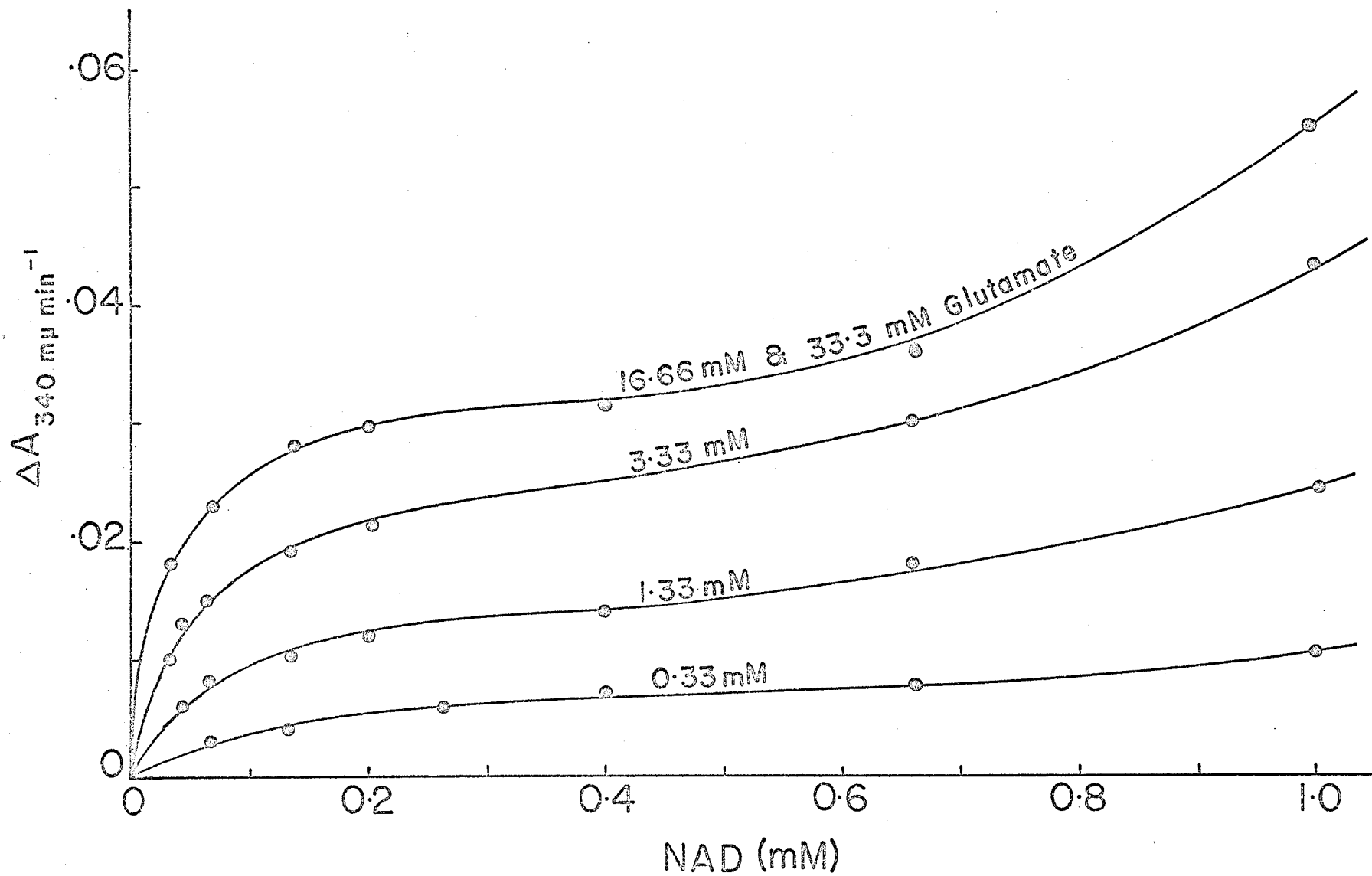
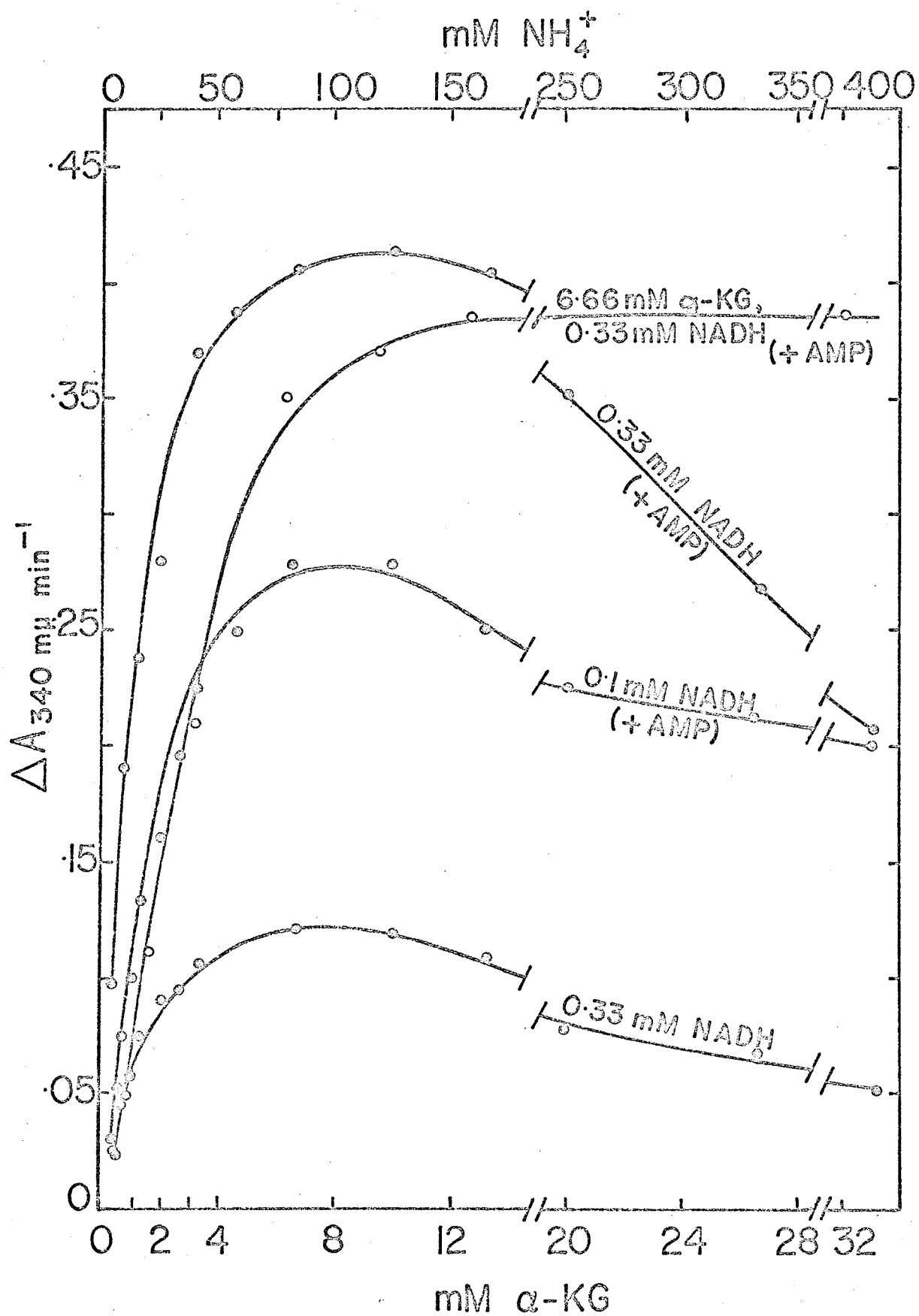


Figure 3. Rate of the reductive amination of  $\alpha$ -ketoglutarate catalysed by Blastocladiella glutamic dehydrogenase as a function of (o) ammonia, and (●)  $\alpha$ -ketoglutarate concentrations. In (●) NADH was held constant at low and optimal levels and ammonium sulphate at high level (400 mM). Reaction mixtures contained 0.2 M Tris-chloride, pH 7; 11  $\mu$ g enzyme protein; 2 mM AMP (saturating) where indicated.



$\alpha$ -ketoglutarate and NADH at high concentrations are themselves very strong inhibitors of the reaction in which they act as substrates. In contradistinction,  $\text{NH}_4^+$  is not inhibitory at extremely high concentrations.

Earlier studies had indicated that glutamic dehydrogenase from various sources was prone to influence by purine nucleotides (8, 14, 27, 52). Therefore, studies were done to determine the effect of purine nucleotides on the rate-concentration patterns of the Blastocladiella enzyme.

The effect of various purine nucleotides on the rate of the oxidative deamination of glutamate is shown in Table II. It is evident that at these concentrations GTP and ATP inhibit the reaction rate considerably while AMP and ADP activate the reaction. Because of their relevance to an 'adenylate control' type of regulation mechanism (see the "Discussion" for an elaboration) AMP (positive) and ATP (negative) effectors were used throughout these kinetic studies.

In the presence of saturating levels of AMP double reciprocal rate-concentration plots for  $\text{NAD}^+$  reduction were linearized. In the case of NADH oxidation saturating levels of AMP did not overcome inhibition by high substrate concentrations. Interactions between AMP and  $\text{NAD}^+$  at a fixed high level of glutamate are shown in Fig. 4. With

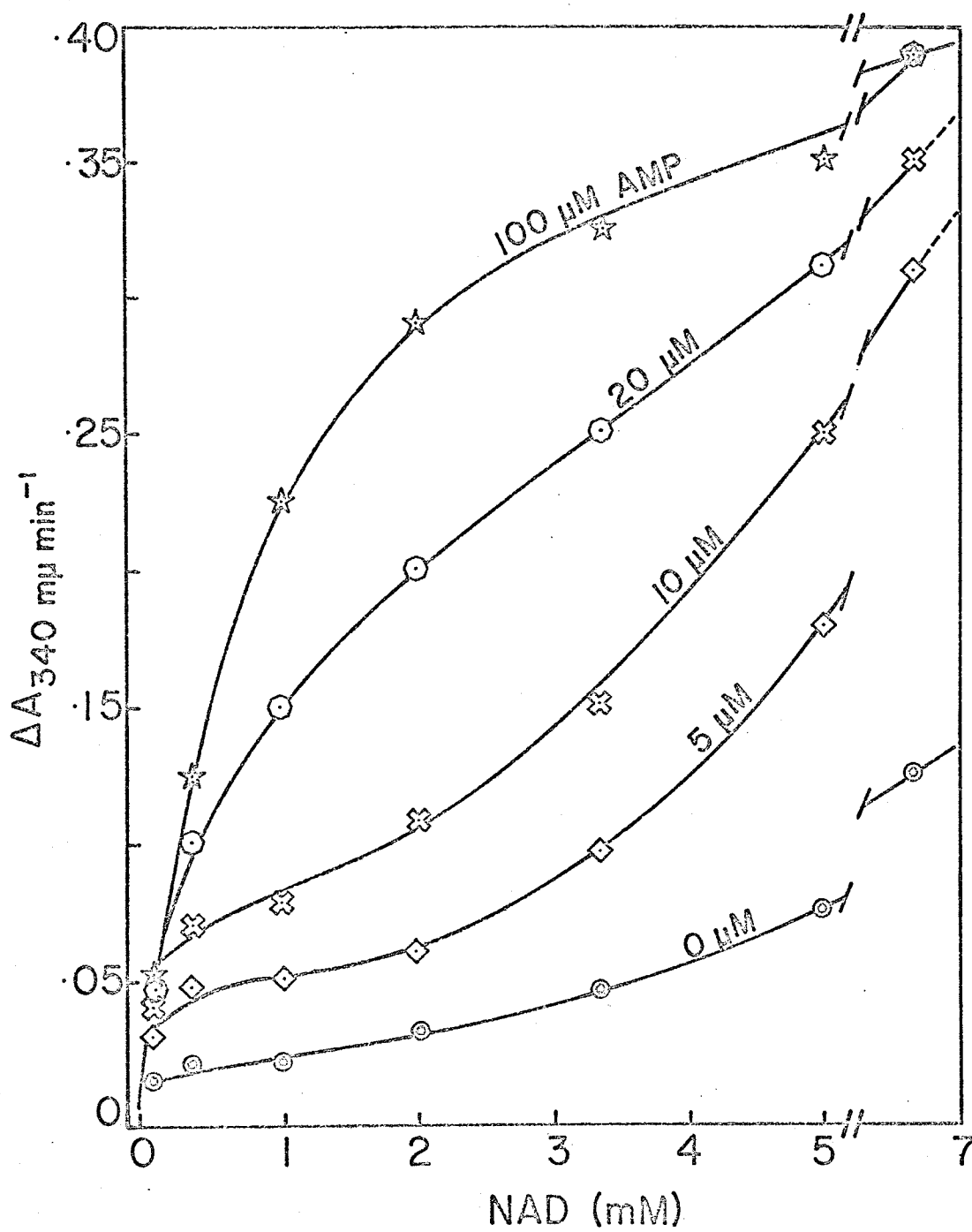
Table II

The effect of various purine nucleotides on the reaction rate of Blastocladiella glutamic dehydrogenase.

The standard reaction mixture contained 50 mM glutamate; 4 mM NAD<sup>+</sup>; 0.2 M Tris-chloride, pH 9; 22  $\mu$ g enzyme protein.

Addition	Concentration mM	Reaction rate
None		0.066
AMP	1.0	0.422
ADP	1.0	0.408
ATP	0.2	0.012
GDP	0.2	0.038
GTP	0.2	0.010
ITP	1.0	0.068
IMP	1.0	0.066
CTP	1.0	0.062
CDP	1.0	0.070

Figure 4. Interactions between the concentration of  $\text{NAD}^+$  and glutamate at several levels of AMP in determining the rate of oxidative deamination of glutamate. Reaction mixtures contained 0.2 M Tris-chloride buffer, pH 9; 20  $\mu\text{g}$  enzyme protein; AMP as indicated; glutamate fixed at 100 mM concentration



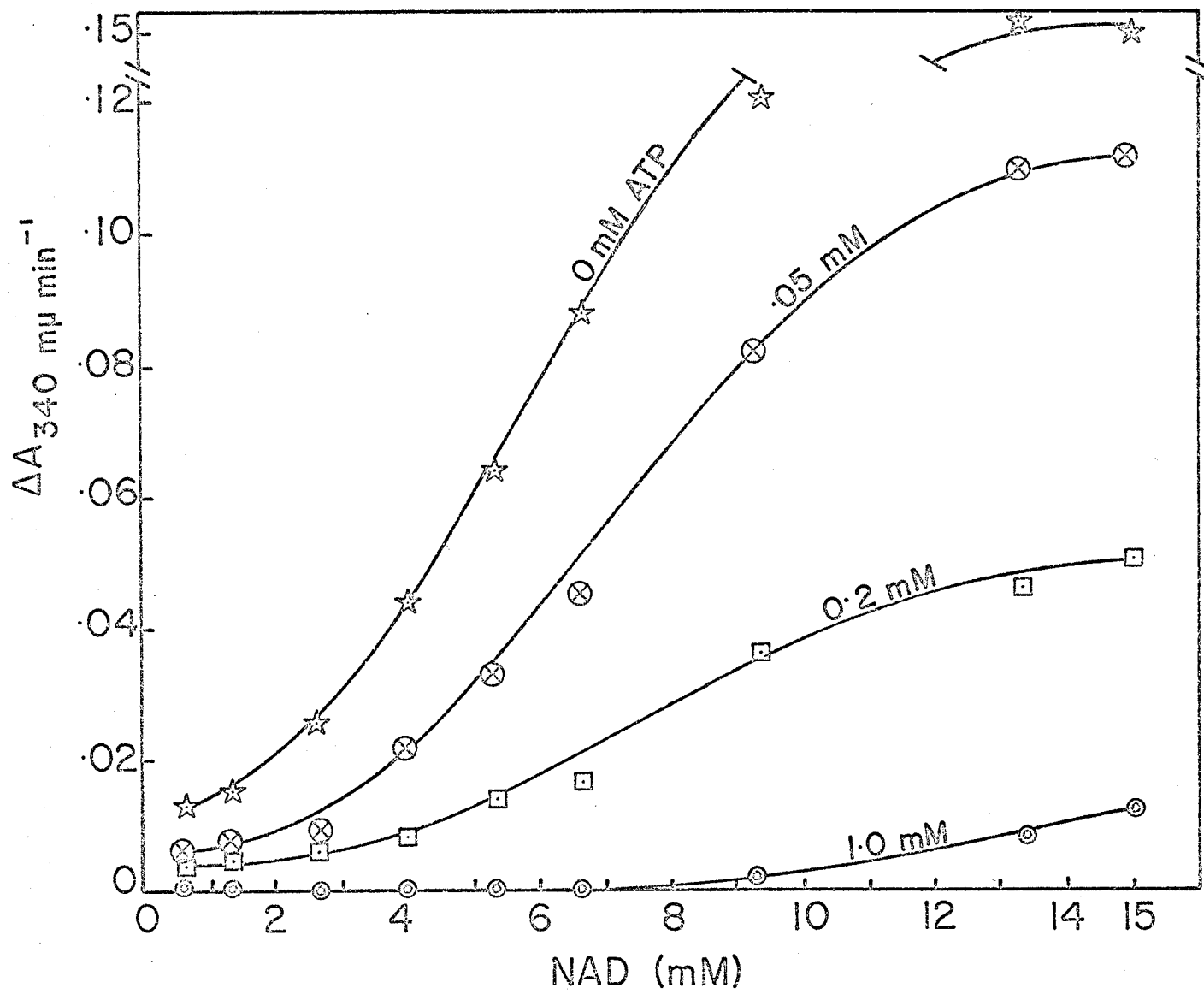
increasing levels of AMP a rapid shift from sigmoid to hyperbolic curves became evident. Therefore, from these rate-concentration plots (Fig. 1 and 4) one must conclude that optimal activity for the oxidative deamination reaction is achieved at very high (probably non-physiological concentrations) of  $\text{NAD}^+$  (20 mM) or at very low levels of  $\text{NAD}^+$  (< 1 mM) in the presence of catalytic amounts of AMP.

The effect of AMP on the reductive amination of  $\alpha$ -ketoglutarate can be seen in Fig. 3. It is apparent that even in the presence of saturating levels of AMP (2 mM) substrate inhibition is still intense. Therefore, the regulatory action of AMP may be of greater significance in the oxidative deamination reaction where kinetic parameters other than activation of the reaction rate have been affected.

The effect of ATP on the reduction of  $\text{NAD}^+$  is seen in Fig. 5. ATP was completely inhibitory at 1 mM concentration. From the curves it can be seen that ATP can abolish the initial hyperbolic response seen at low substrate concentrations (Fig. 2). The antagonistic interaction between  $\text{NAD}^+$  and ATP is clear.

Since AMP and ATP act in opposition from the kinetics observed so far, it was of interest to study their interaction

Figure 5. Interactions between  $\text{NAD}^+$  and glutamate at several fixed levels of ATP in determining the rate of the oxidative deamination of glutamate. Reaction mixtures contained 0.2 M Tris-chloride buffer, pH 9; 25  $\mu\text{g}$  enzyme protein; ATP as indicated; glutamate fixed at 50 mM concentration.



under conditions where substrate ligands are non-saturating. Rate-concentration plots were obtained with AMP as the variable substrate and ATP at several fixed concentrations.  $\text{NAD}^+$  and glutamate were at fixed concentrations. In the absence of ATP the rate-concentration profile was hyperbolic as expected. With increasing concentrations of ATP, the curves became increasingly sigmoidal. This observation lent support to the description of plots in Fig. 1a as being largely sigmoidal. When plotted in double reciprocal form the data yielded parabolic plots which appeared to extrapolate to the same  $V_{\text{max}}$ . AMP and ATP, therefore, showed clear competitive inhibition.

A further analysis of this data by the recent computer-based procedure proposed by Frieden (15) was made. This method depends upon conversion of the binding equation of Monod et al (43) for fractional saturation ( $\bar{Y}$ ) of a protein with a ligand.

$$\text{i.e., } \bar{Y} = \frac{\alpha(1 + \alpha)^{n-1} + Lc\alpha(1 + c\alpha)^{n-1}}{(1 + \alpha)^n + L(1 + c\alpha)^n}$$

where  $\underline{L}$  = the equilibrium constant between two conformational states;  $\underline{c}$  = the difference in the ability of the two states to bind the ligand;  $\underline{n}$  = the number of ligand binding sites

per mole of protein, and;  $\alpha$  = the reduced ligand concentration (i.e., the concentration of unbound ligand divided by a binding constant (K) for the conformation of protein which binds the ligand tightest) to a kinetic equation. This conversion is accomplished by replacing  $\bar{Y}$  with  $v_0/n V_{\max}$ . Therefore

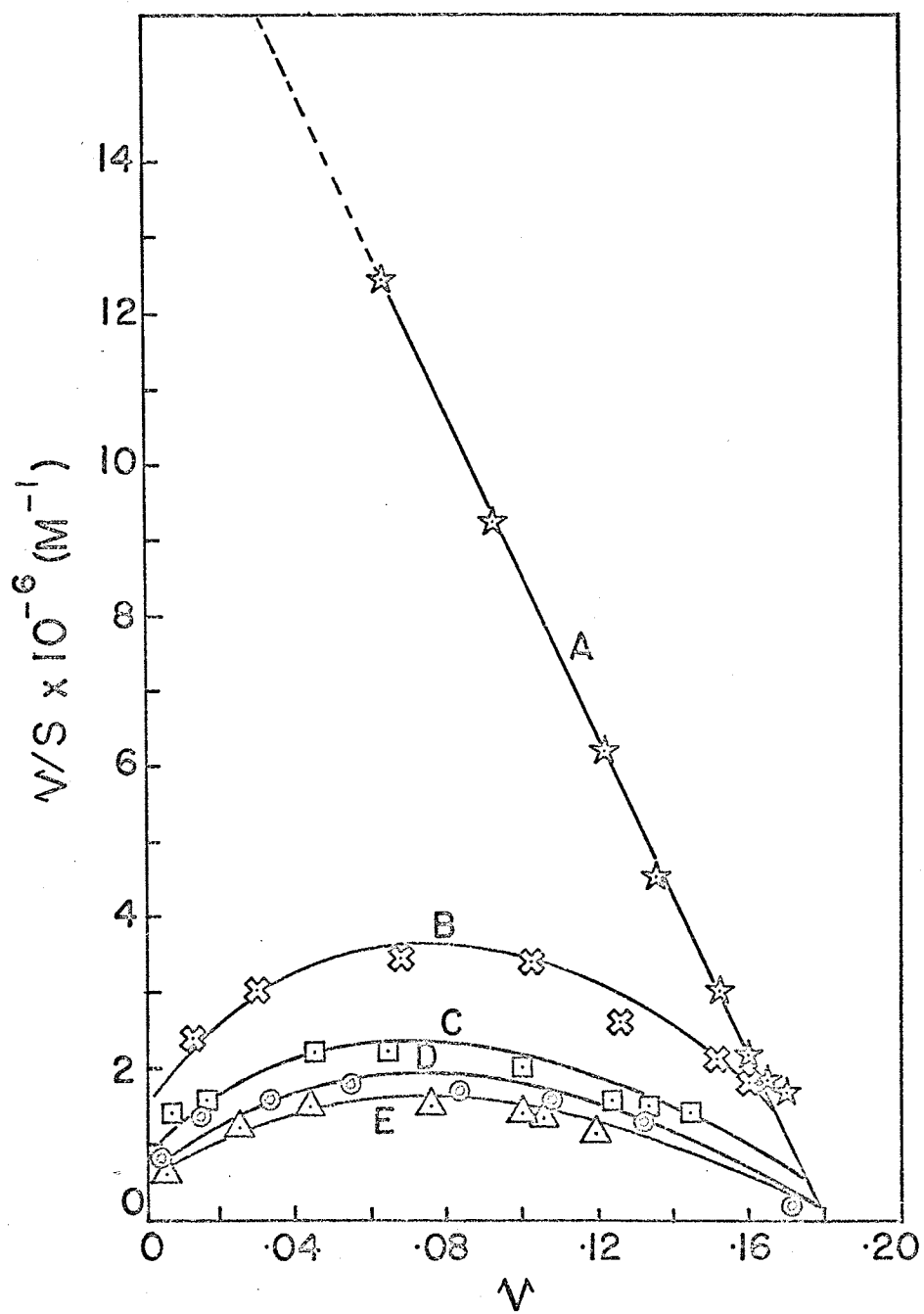
$$\frac{v_0}{n V_{\max}} = \frac{\alpha(1 + \alpha)^{n-1} + Lc\alpha(1 + c\alpha)^{n-1}}{(1 + \alpha)^n + L(1 + c\alpha)^n}$$

where  $v_0$  = the initial velocity and  $V_{\max}$  is the maximum initial velocity. One may plot  $v/s$  against  $v$  at different modifier levels and thus obtain 'binding-type' curves. With such a technique the data in Fig. 6 were obtained. (Curves have been fitted by eye rather than by computer.) Comparing these curves with the theoretical and experimental plots of Frieden (15) an  $n$  value of 4 could be estimated with  $c$  and  $L$  values similar to those calculated for deoxythymidine diphosphate-D-glucose pyrophosphorylase (15). It is interesting to observe that the Hill plot interaction coefficient was estimated with a maximum value of 2.

#### I. B. Determination of Michaelis constants

Despite the irregularities found with rate-concentration plots, attempts were made to evaluate kinetic constants.

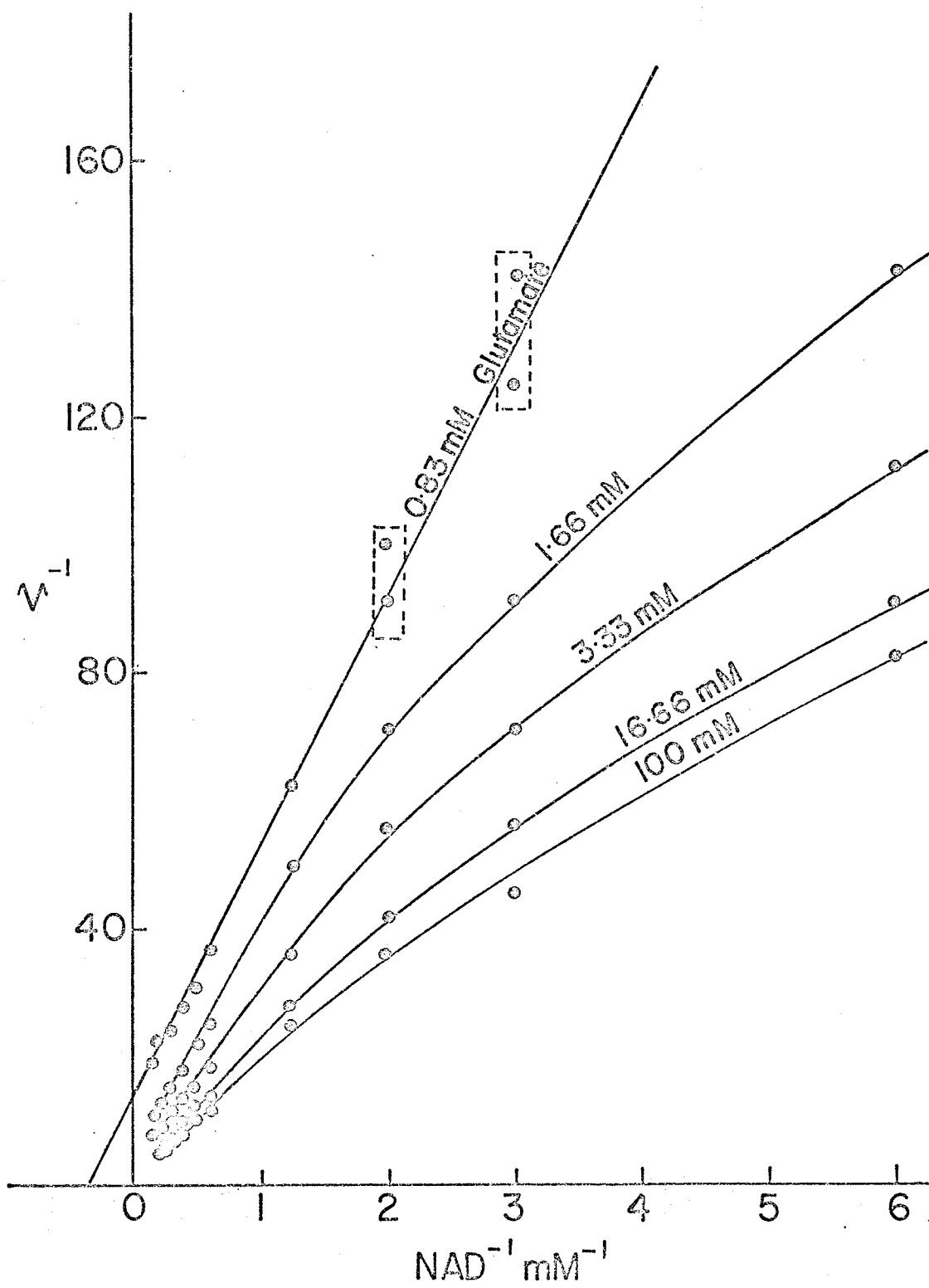
Figure 6. Interactions between allosteric modifiers (AMP and ATP) at fixed levels of glutamate and  $\text{NAD}^+$  (AMP the variable substrate) plotted as v/s against v. Levels of ATP used were: (A) 0 mM; (B) 1 mM; (C) 2.5 mM; (D) 5 mM; and (E) 10 mM. Reaction mixtures contained 0.2 M Tris-chloride, pH 9; 12  $\mu\text{g}$  enzyme protein; 50 mM glutamate; 2.66 mM  $\text{NAD}^+$ .



The Michaelis constant ( $K_m$ ) is a kinetically defined quantity that represents the concentration of substrate which half-saturates the enzyme, i.e., the substrate concentration at one-half  $V_{max}$ .  $V_{max}$  is defined as the maximal initial velocity. The Michaelis-Menten equation is as follows:  $v = \frac{V_a}{K_a + a}$  where  $v$  = initial velocity;  $a$  = substrate concentration;  $V_a = V_{max}$  (as defined above); and  $K_a = K_m$  (as defined above). A knowledge of the values of  $V_{max}$  and  $K_m$  is necessary and sometimes, is sufficient to describe a rate equation.

One very common method of estimating  $K_m$  is the Lineweaver-Burk method of transposing the hyperbolic equations of Michaelis to a straight line equation by the use of reciprocals of the reaction rate and varied substrate concentrations. If a mechanism does not include alternate reaction sequences, and no substrate reacts with more than one enzyme form, then, according to Cleland's analysis (6) a replot of intercepts against reciprocal concentrations of changing fixed substrate must be linear. Analysis of slope effects, however, may or may not show a reversible connection between enzyme forms combining with the variable and fixed changing substrate. Therefore, two possible patterns may exist: parallel lines when no reversible

Figure 7. Double reciprocal plots of rate of oxidative deamination of glutamate against  $\text{NAD}^+$  concentration. Glutamate levels were as indicated. Reaction mixtures contained 0.2 M Tris-chloride buffer, pH 9; 44  $\mu\text{g}$  enzyme protein.



connection exists or lines intersecting to the left of the vertical axis when forms are reversibly connected. A replot of slopes against reciprocal concentration of changing fixed substrate is linear.

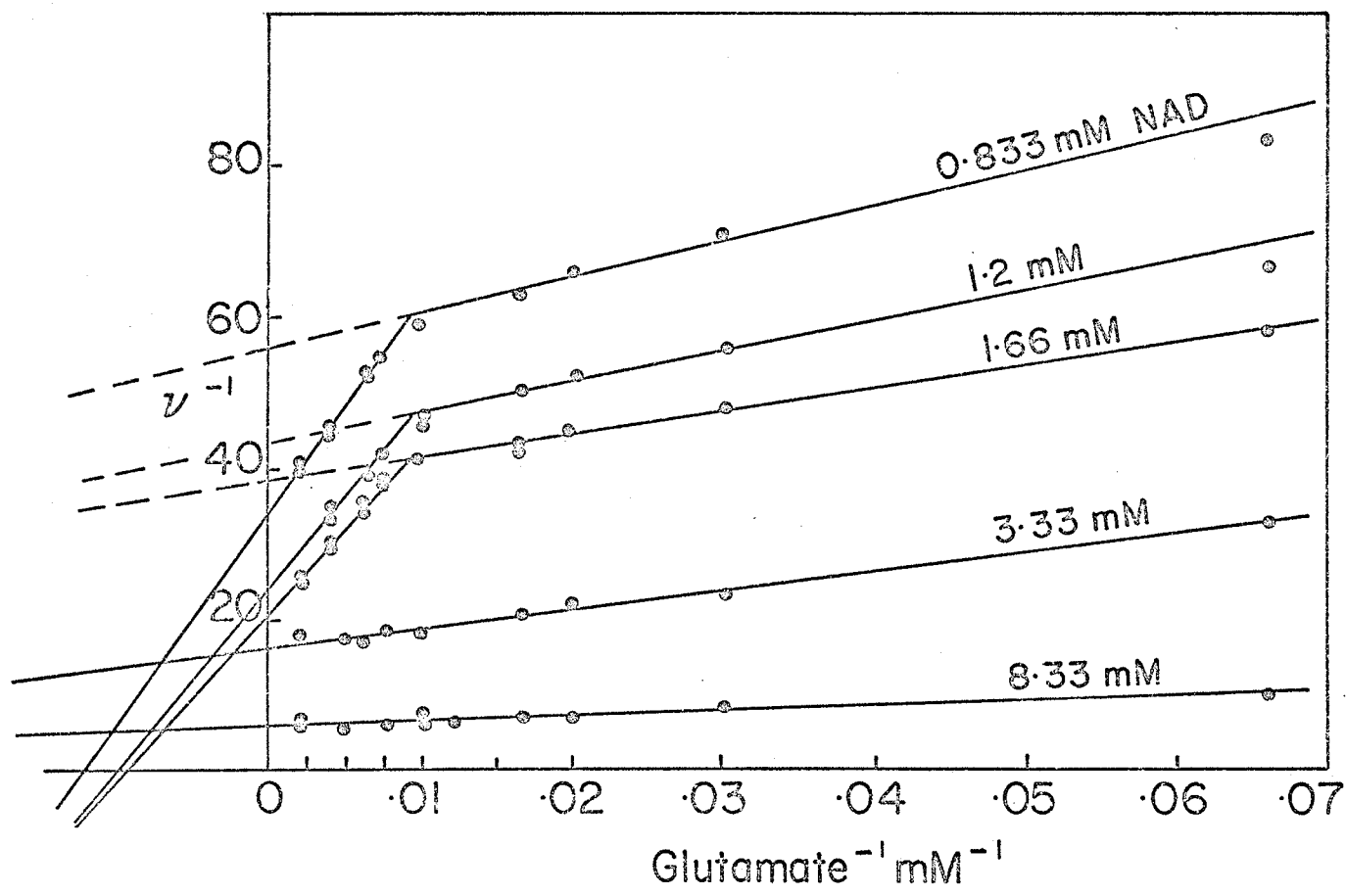
Double reciprocal plots for the oxidative deamination of glutamate were complex (Fig. 7). By careful selection of concentrations, biphasic plots (two portions with significantly different slopes) were obtained (Fig. 7 and 8). The data from Fig. 8 would tend to support Frieden's interpretation (8) that two  $\text{NAD}^+$  binding sites are present. One would be the active site and the other an allosteric site. This is implicit in the equation derived by Frieden (11):

$$v = \frac{V_1 + V_2 \frac{\text{NAD}^+}{K_2}}{1 + \frac{K_1}{\text{NAD}^+} + \frac{\text{NAD}^+}{K_2}}$$

where  $K_1$  and  $K_2$  are Michaelis constants for  $\text{NAD}^+$  at the two respective sites and  $V_1$  and  $V_2$  are maximum velocities when one site (active site) or both sites are filled.

The double reciprocal plots of Fig. 8, however, indicate that glutamate is also an activator. This is evident at relatively low  $\text{NAD}^+$  concentrations. This would explain why saturation curves for glutamate appear hyperbolic. Thus, very high glutamate levels may be necessary to

Figure 8. Double reciprocal plots of rate of the oxidative deamination of glutamate against glutamate concentration.  $\text{NAD}^+$  levels as indicated. Reaction mixtures contained 0.2 M Tris-chloride buffer, pH 9; 22  $\mu\text{g}$  enzyme protein.



produce saturation curves of the type described when  $\text{NAD}^+$  is the variable substrate (Fig. 1a and 2). Substrate analogues of glutamate were ineffective in enhancing glutamate activation (30). These irregularities serve to emphasize the inaccuracy in the calculation of  $K_{m1}$  (Michaelis constant) and  $K_{m2}$  (activation constant) for  $\text{NAD}^+$  and glutamate (Table III).

The kinetic constants for the reductive amination of  $\alpha$ -ketoglutarate were also difficult to assess as high concentrations of NADH and  $\alpha$ -ketoglutarate were extremely inhibitory. By choosing non-inhibitory levels of NADH and  $\alpha$ -ketoglutarate the double reciprocal plots in Fig. 9 were obtained. From replots of this data, the Michaelis constants for NADH and  $\alpha$ -ketoglutarate could be calculated (Table III).

The effect of purine nucleotides on the enzyme has already been described. The indications were that AMP altered the complex plots of the oxidative deamination reaction into normal Michaelian-type curves. Therefore, the double reciprocal plots obtained were derived in the presence of saturating levels of AMP so that proper  $K_m$ 's could be calculated. In the presence of AMP double reciprocal plots for the oxidative deamination reaction were linearized (Fig. 10) and a single  $K_m$  could be determined for each substrate. The  $K_m$  for glutamate increased four-fold while the  $K_m$  for  $\text{NAD}^+$  decreased slightly. These

Figure 9. Double reciprocal plots of rate of the reductive amination of  $\alpha$ -ketoglutarate against NADH concentration. Reaction mixtures contained 0.2 M Tris-chloride buffer, pH 7; 11  $\mu$ g enzyme protein; ammonia 400 mM;  $\alpha$ -ketoglutarate as indicated.

Inset: Replot of intercepts against reciprocal  $\alpha$ -ketoglutarate concentration.

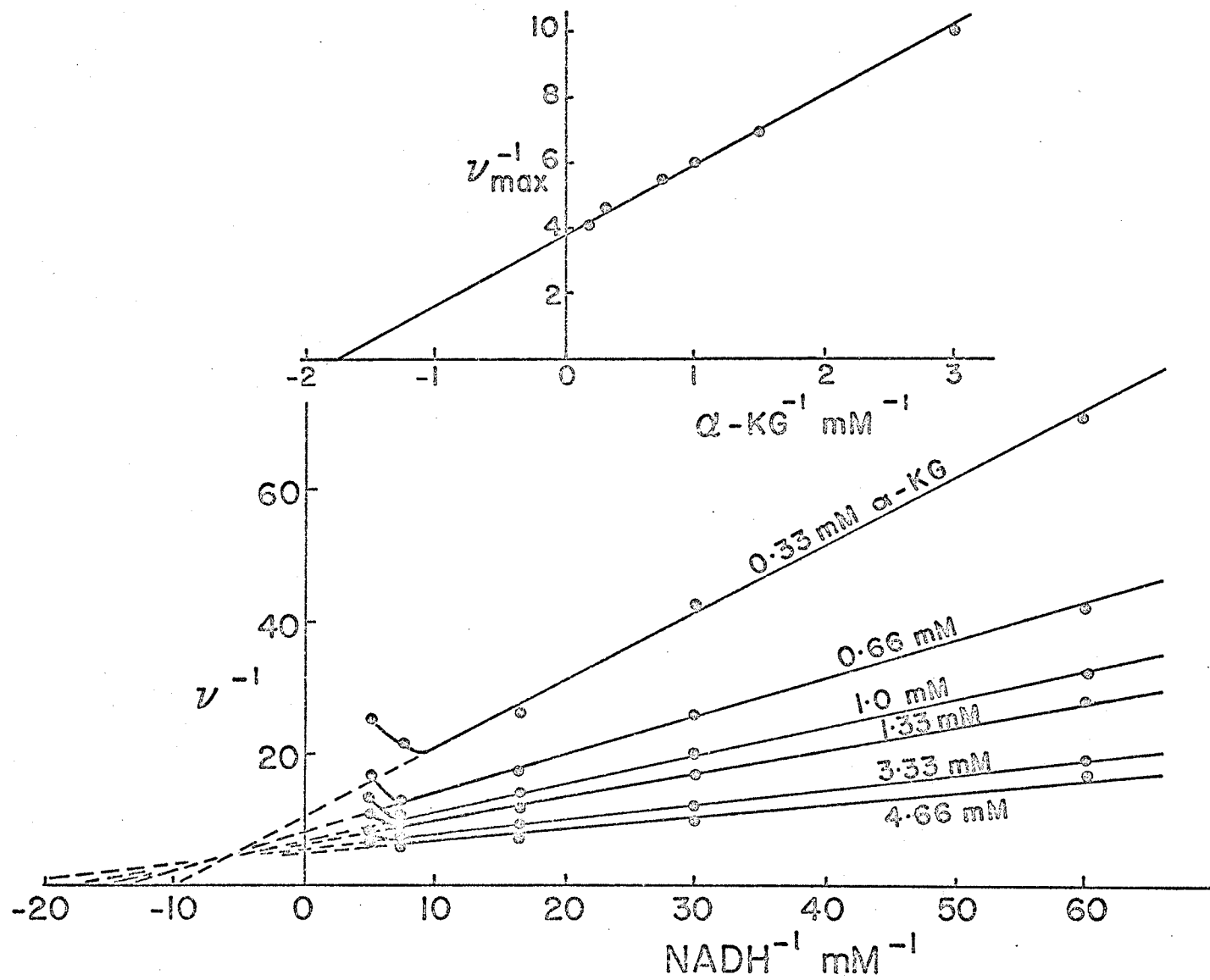


Figure 10. Double reciprocal plots of the rate of the oxidative deamination of glutamate against  $\text{NAD}^+$  concentration. Reaction mixtures contained 0.2 M Tris-chloride buffer, pH 9; AMP 1 mM; glutamate as indicated; 22  $\mu\text{g}$  enzyme protein. Inset: Replot of intercept against reciprocal glutamate concentration.

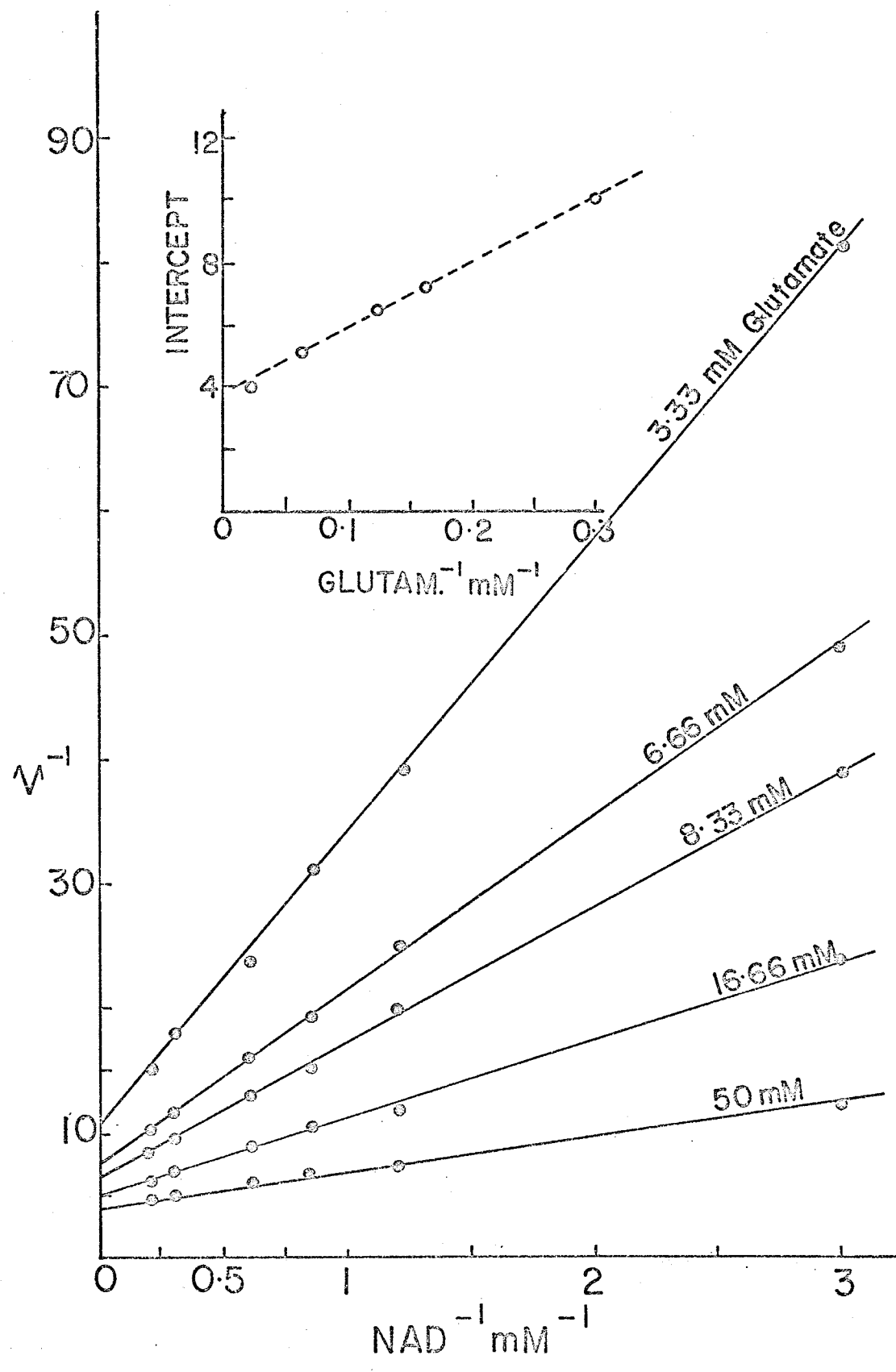


Table III

Kinetic constants of substrates and effector of Blastocladiella glutamic dehydrogenase

Substrate	Kinetic Constants			
	(-AMP)		(AMP)	
	$K_{m1}$	$K_{m2}$	$K_{m3}$	$K_i$
L-glutamate	$1.43 \times 10^{-3}$ M	$13.3 \times 10^{-3}$ M	$5.7 \times 10^{-3}$ M	-
NAD <sup>+</sup>	$4.0 \times 10^{-4}$ M	$2.0 \times 10^{-3}$ M	$3.0 \times 10^{-4}$ M	-
$\alpha$ -ketoglutarate	$5.6 \times 10^{-4}$ M	-	$6.6 \times 10^{-4}$ M	$3.0 - 10.0 \times 10^{-3}$ M
NADH	$3.3 \times 10^{-5}$ M	-	$3.0 \times 10^{-4}$ M	$1.6 \times 10^{-5}$ M
Ammonia	$4.0 \times 10^{-2}$ M	-	$4.0 \times 10^{-2}$ M	$3 \times 10^{-3}$ M
AMP	20 $\mu$ M	-	-	-

changes are significant but the possibility exists that the differences arose from the difficulty of assessing kinetic constants from the biphasic plots (Fig. 7 and 8).

For the reductive amination reaction, however, saturating levels of AMP failed to overcome substrate inhibition (Fig. 11). In the presence of saturating AMP  $K_m$  values for  $\text{NH}_4^+$  and  $\alpha$ -ketoglutarate were unchanged. The  $K_m$  for NADH, however, increased ten-fold. Further implications of this AMP effect will be elucidated in the "Discussion".

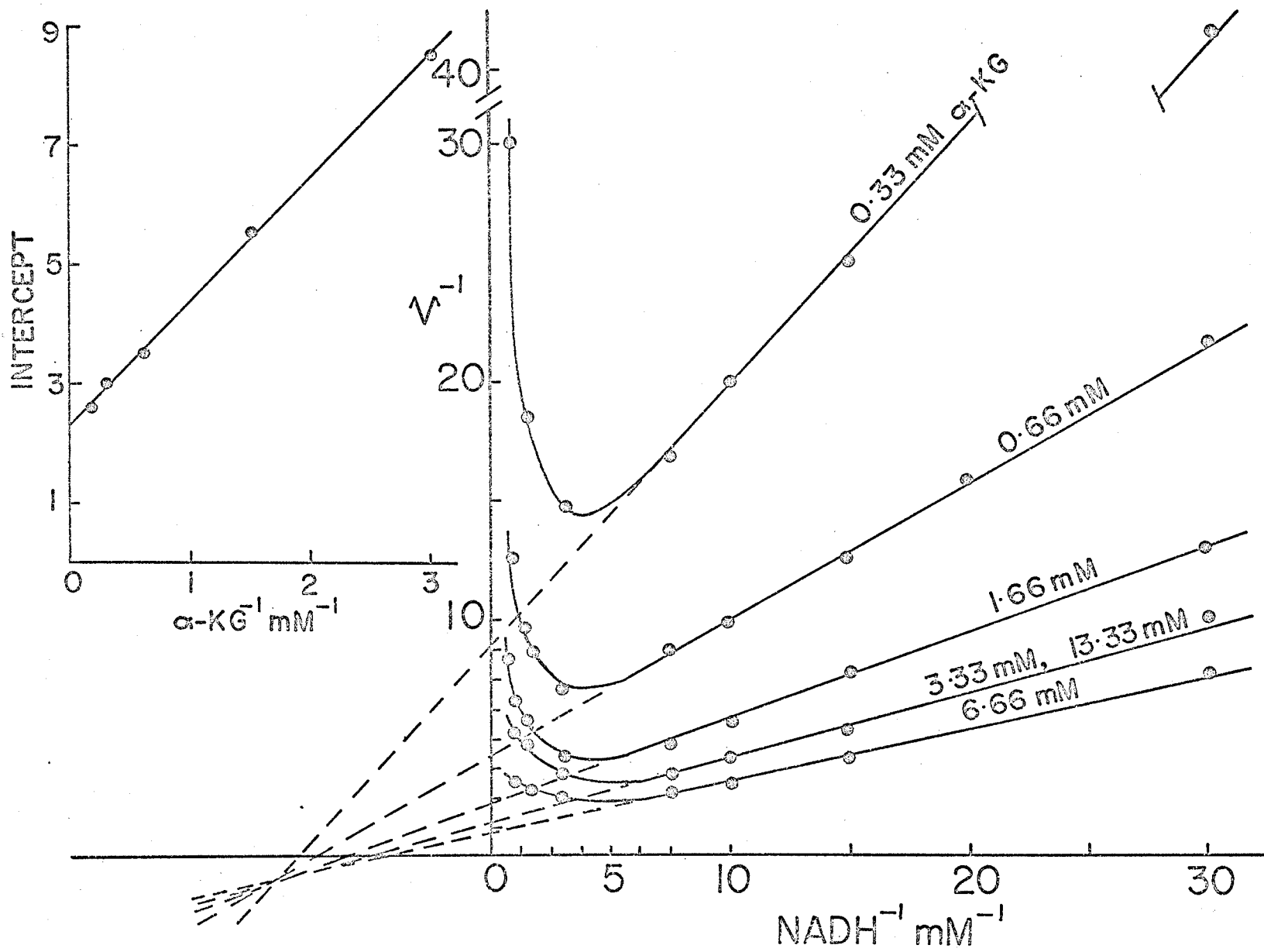
## II. A. Product Inhibition Studies

In order to enhance the formulation of a kinetic mechanism of enzyme action product inhibition studies were carried out. The nomenclature of the reaction mechanism and the description of the kinetic constants are those proposed by Cleland (6).

Product inhibition studies were used to determine inhibition constants, sequence of substrate addition, and product release. All such studies were carried out for the oxidative deamination reaction in the presence of AMP so as to obtain linear plots. From double reciprocal plots, replots of slopes or intercepts against inhibitor concentration were made.

Figure 11. Double reciprocal plots of rate of the reductive amination of  $\alpha$ -ketoglutarate against NADH concentration. Reaction mixtures contained 0.2 M Tris-chloride buffer, pH 7; ammonium sulphate 400 mM; AMP 2 mM (saturating);  $\alpha$ -ketoglutarate as indicated; 12  $\mu$ g enzyme protein.

Inset: Replot of intercepts against reciprocal  $\alpha$ -ketoglutarate concentration.



In the case of competitive inhibition product inhibition constants were calculated from the point of intersection with the horizontal axis of a replot of slope against inhibitor concentration. For non-competitive inhibition a replot of slopes against inhibitor concentration gives a point of intersection on the horizontal axis of  $-K_i \left(1 + \frac{X}{K_x}\right)$  and a replot of intercept  $\left(\frac{1}{v}\right)$  against inhibitor concentration gives a point  $-K_i \left(1 + \frac{X}{K_x}\right)$  where  $X$  = the concentration of the non-varied substrate;  $K_x$  = Michaelis constant of  $X$ ;  $K_{ix}$  = the inhibition constant of  $X$ ; and  $K_i$  = the inhibition constant of the product inhibitor.

When dealing with uncompetitive inhibition, a replot of intercept against inhibitor concentration gives an intersection point on the horizontal axis equal to  $-K_i$ .

With NADH as inhibitor, at several fixed concentrations, and  $\text{NAD}^+$  as the variable substrate (glutamate fixed at a high level -  $20 \times K_m$ ) plots were competitive (Fig. 12). Replot of slopes against NADH concentration gave a linear relationship. The inhibition constant was evaluated (Table III). This pattern would tend to indicate that  $\text{NAD}^+$  and NADH combine with the same enzyme form.

Using ammonium sulphate ( $\text{NH}_4^+$ ) as inhibitor with glutamate fixed ( $20 \times K_m$ ) and  $\text{NAD}^+$  as the variable substrate,

Figure 12. Product inhibition by NADH. Double reciprocal plots of rate of oxidative deamination of glutamate against  $\text{NAD}^+$  concentration. Reaction mixtures contained 0.2 M Tris-chloride buffer, pH 9; AMP 1 mM; glutamate 100 mM; NADH as indicated; 100  $\mu\text{g}$  enzyme protein.

Inset: Replot of slope against NADH concentration.

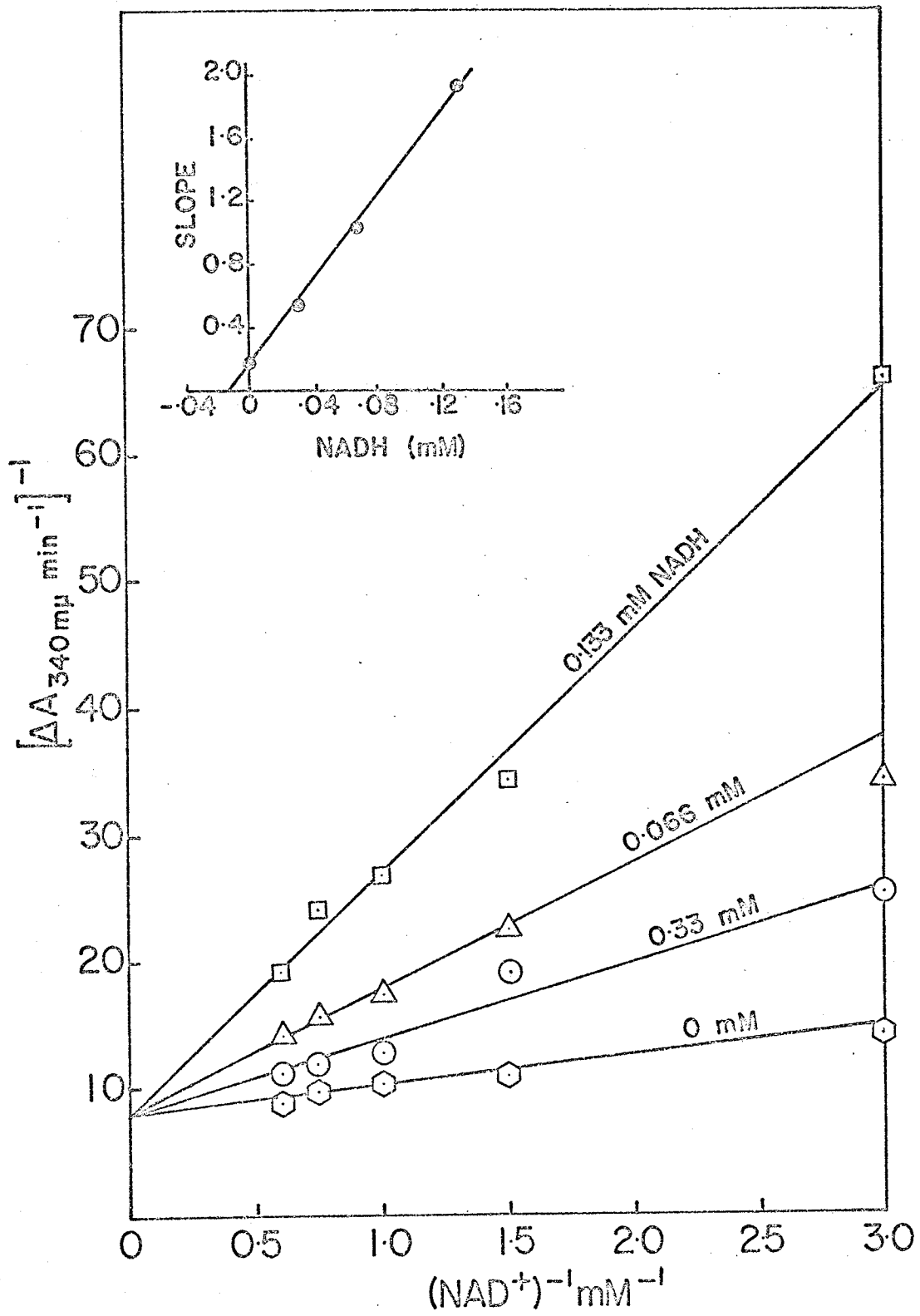


Figure 13. Product inhibition by  $\text{NH}_4^+$ . Double reciprocal plots of rate against  $\text{NAD}^+$  concentration. Reaction mixtures contained 0.2 M Tris-chloride buffer, pH 9; AMP 1 mM; glutamate 100mM;  $\text{NH}_4^+$  as indicated; 100 $\mu\text{g}$  enzyme protein. Inset: Replot of intercept and slope against  $\text{NH}_4^+$  concentration.

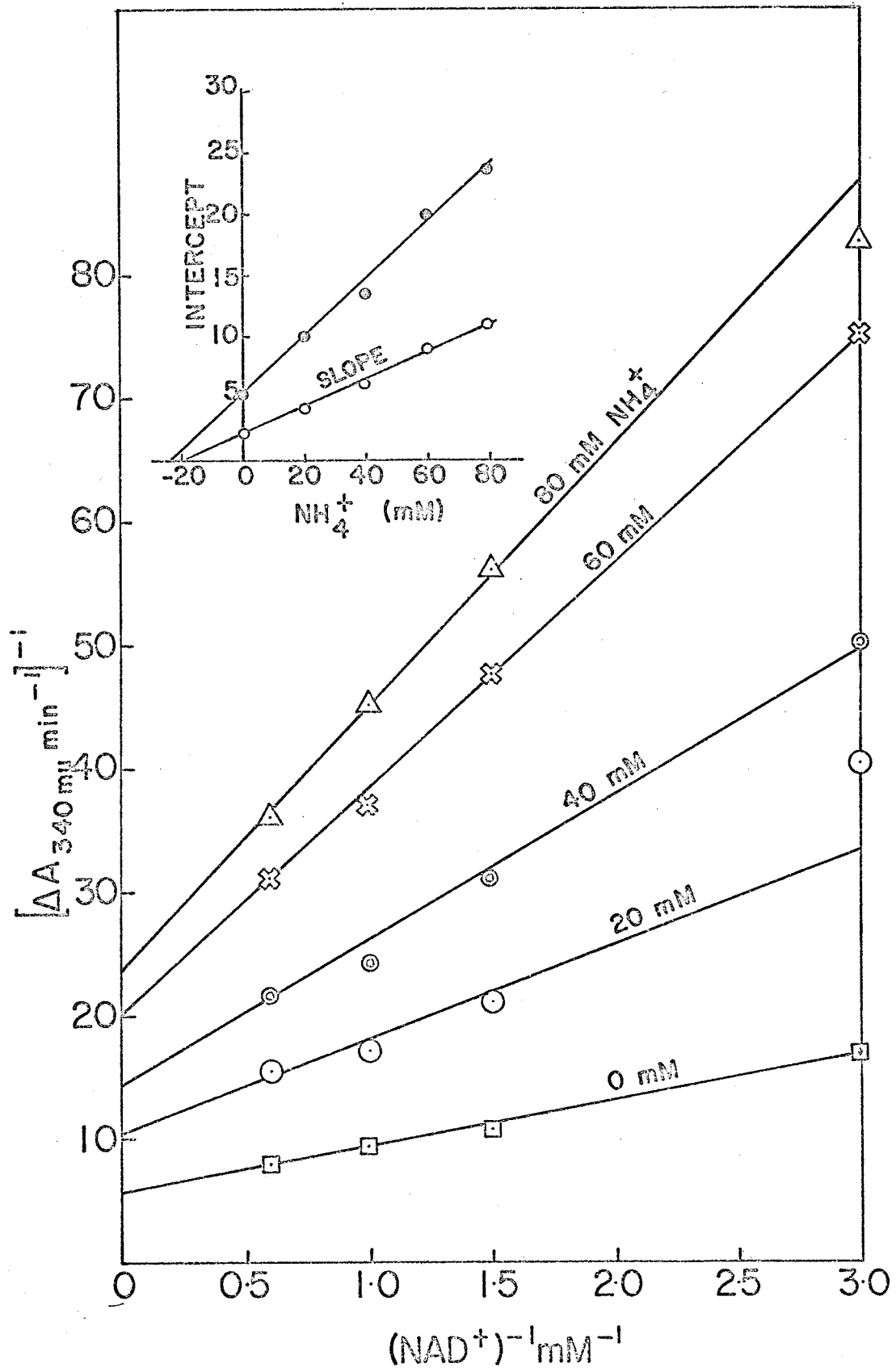


Figure 14. Product inhibition by  $\text{NH}_4^+$ . Double reciprocal plots of rate against  $\text{NAD}^+$  concentration. Reaction mixtures contained 0.2 M Tris-chloride, pH 9; AMP 1 mM; glutamate 200 mM; ammonium sulphate as indicated; 50  $\mu\text{g}$  enzyme protein. Inset: Replot of intercept against  $\text{NH}_4^+$  concentration.

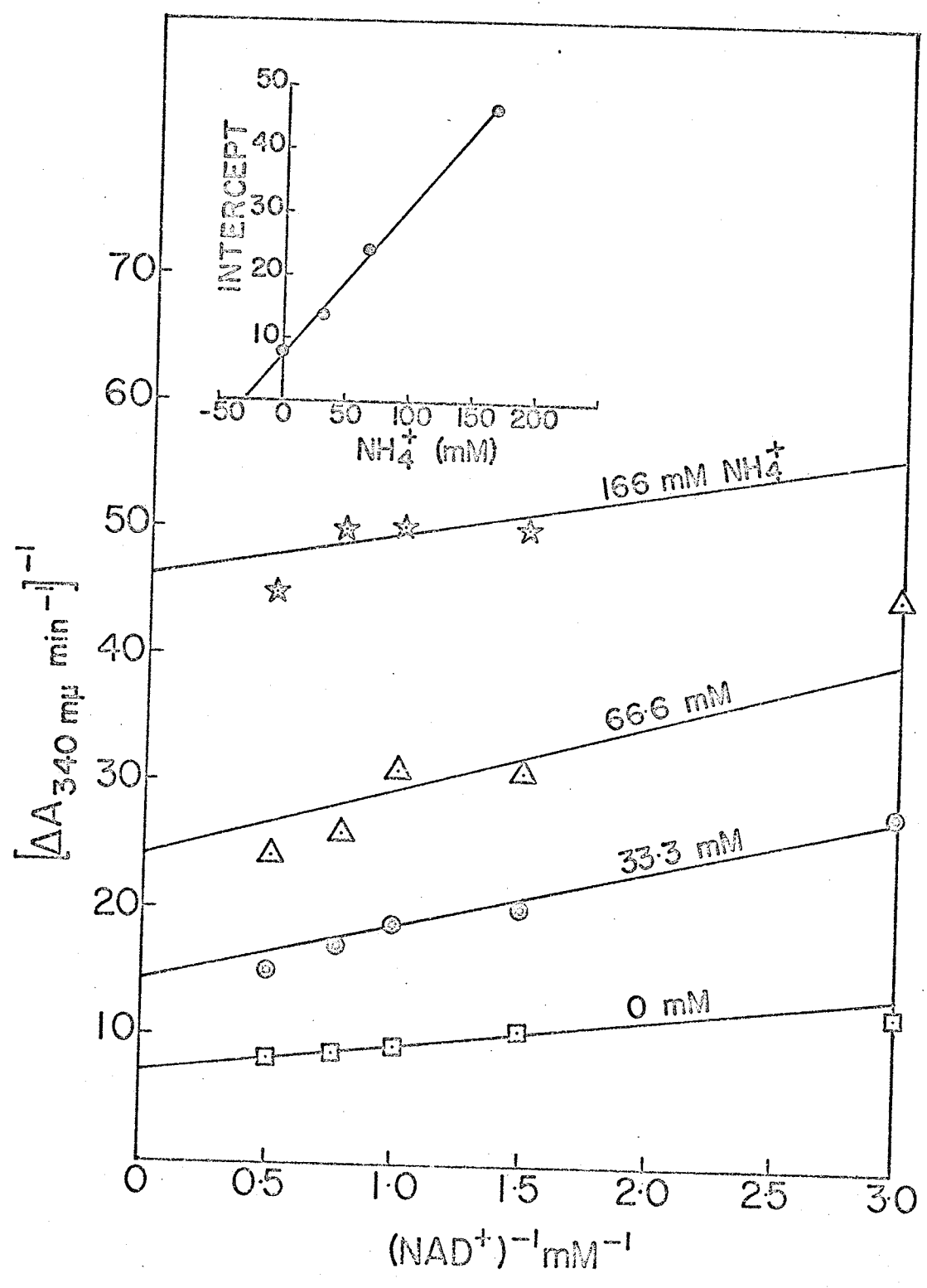


Figure 15. Product inhibition by  $\text{NH}_4^+$ . Double reciprocal plots of rate against glutamate concentration. Reaction mixtures contained 0.2 M Tris-chloride, pH 9; AMP 2 mM;  $\text{NAD}^+$  4 mM; ammonium sulphate as indicated; 100 $\mu\text{g}$  enzyme protein.

Inset: Replot of slope and intercept against  $\text{NH}_4^+$  concentration

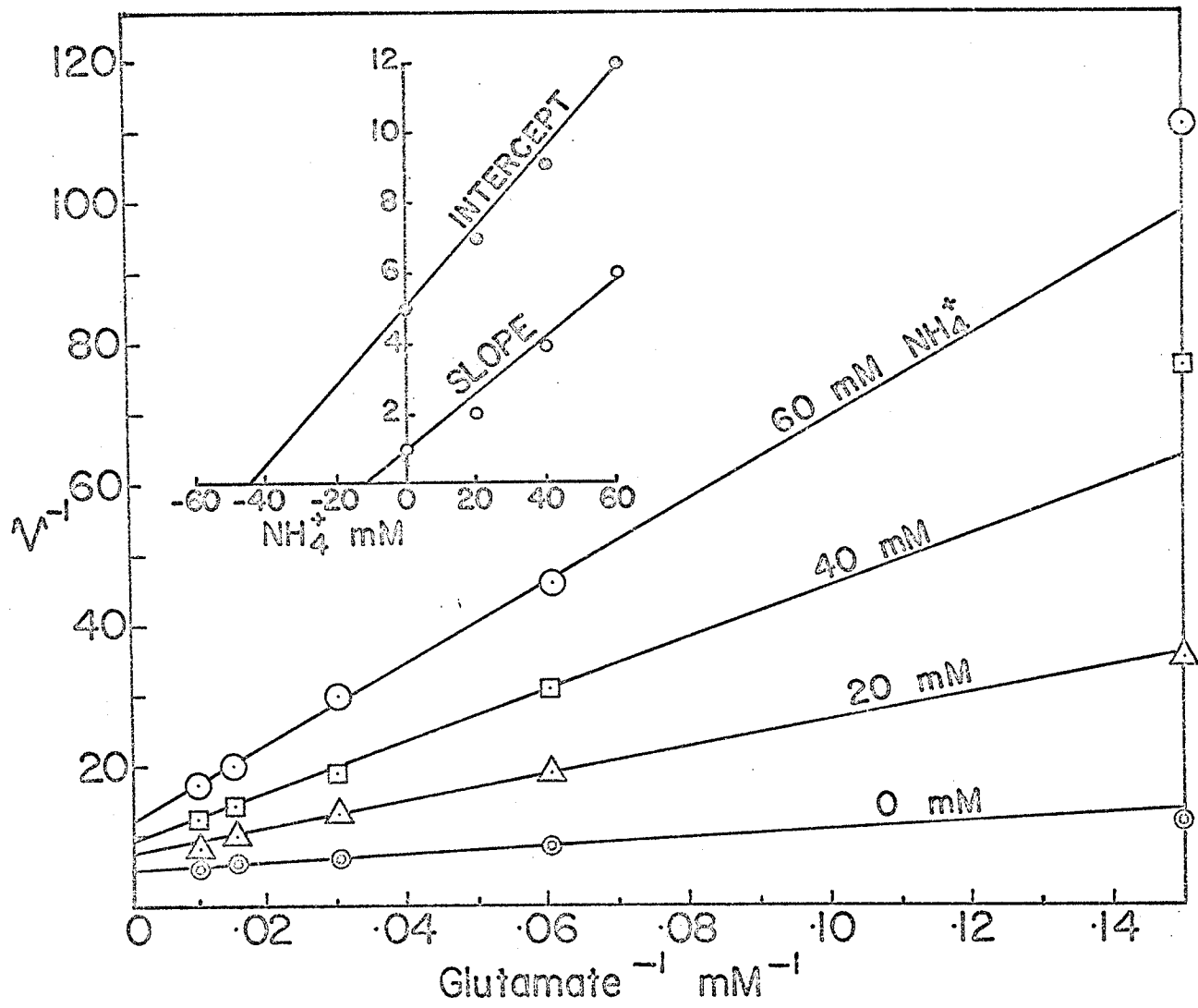


Figure 16. Product inhibition by  $\alpha$ -ketoglutarate.  
Double reciprocal plots of rate against  $\text{NAD}^+$   
concentration. Reaction mixtures contained  
0.2 M Tris-chloride, pH 9; AMP 1 mM;  
glutamate 100mM;  $\alpha$ -ketoglutarate as indicated;  
100 $\mu$ g enzyme protein.  
Inset: Replot of intercept against  $\alpha$ -ketoglutarate  
concentration.

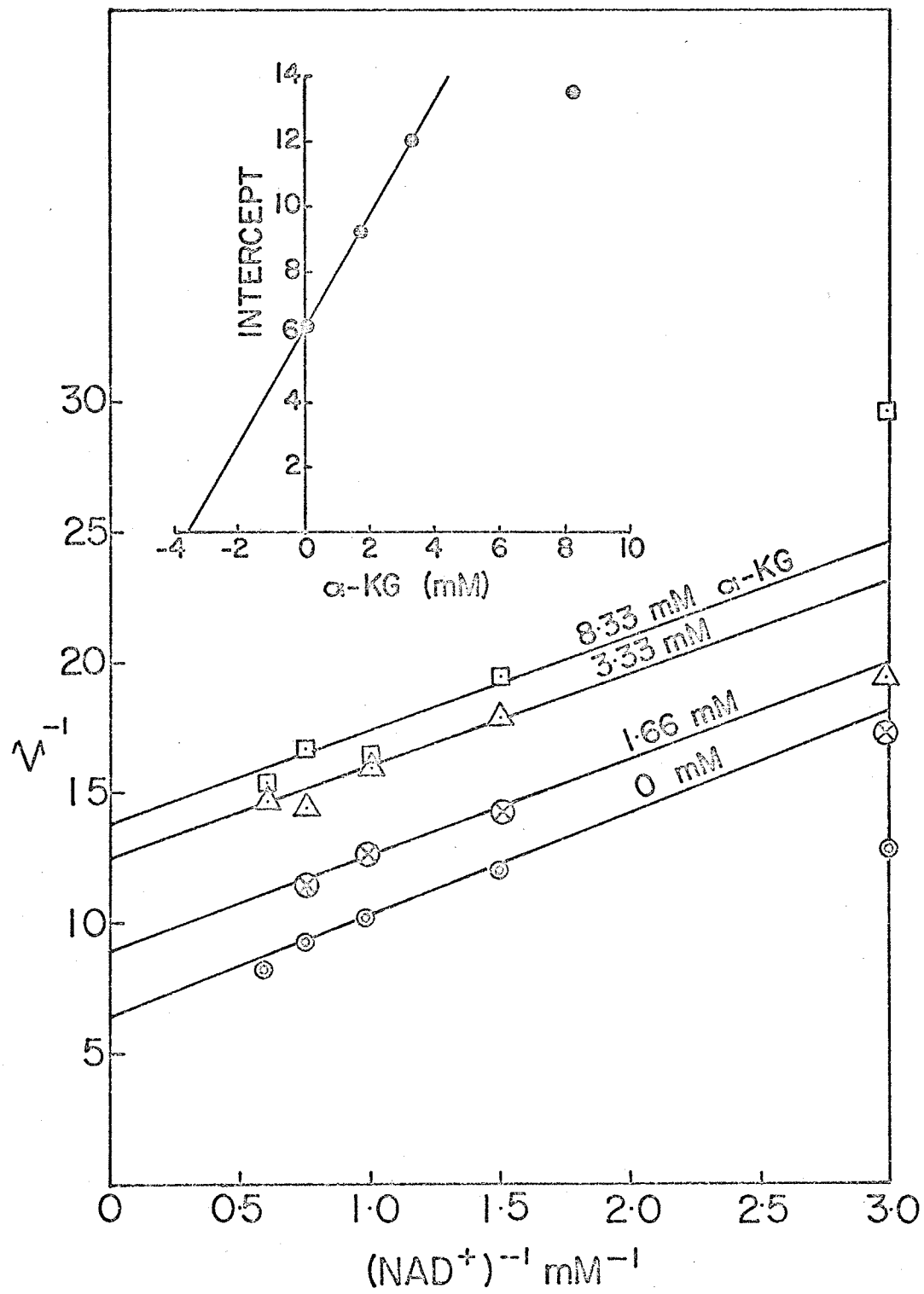
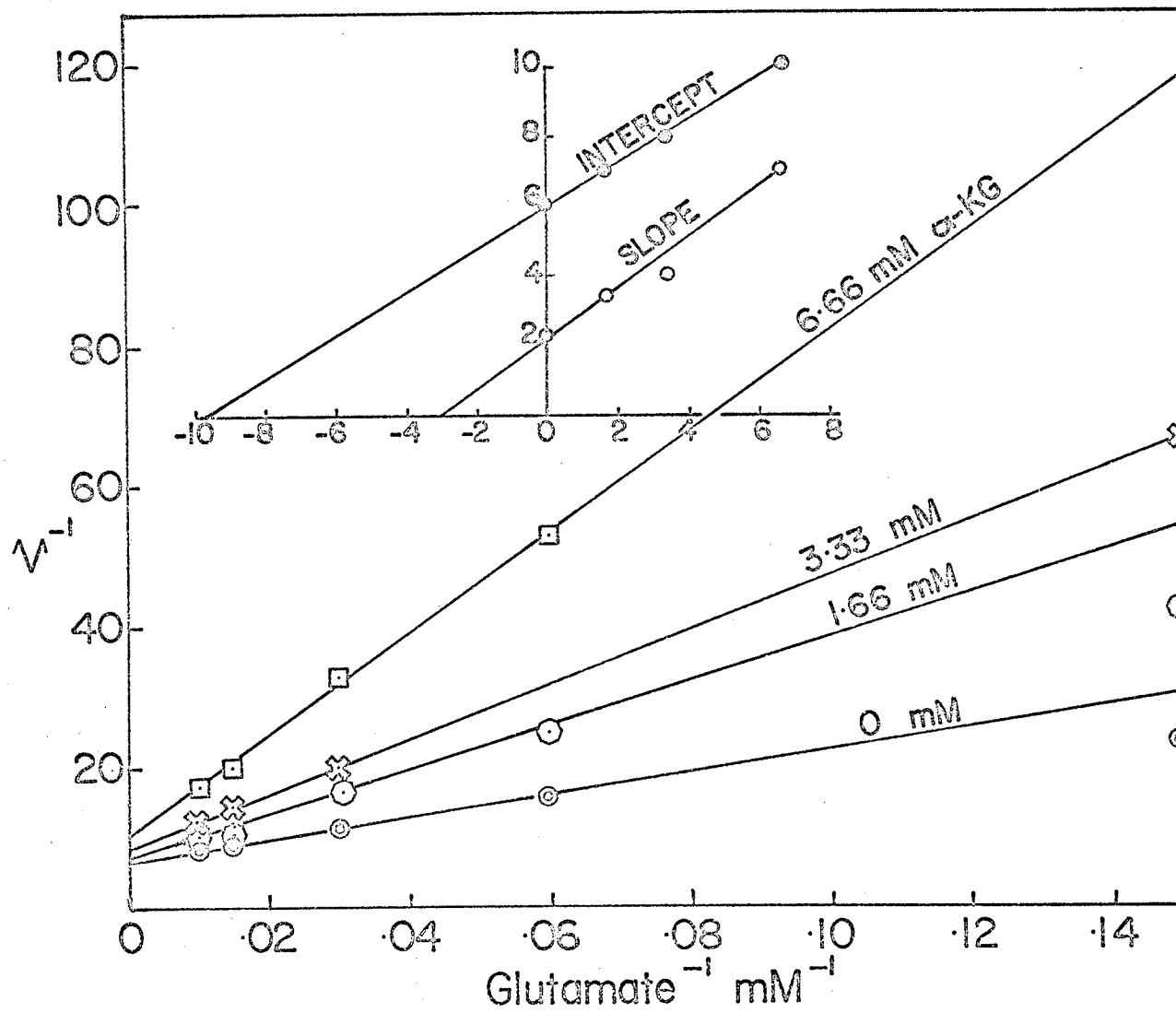


Figure 17. Product inhibition by  $\alpha$ -ketoglutarate. Double reciprocal plots of rate against glutamate concentration. Reaction mixtures contained 0.2 M Tris-chloride, pH 9; AMP 2 mM;  $\text{NAD}^+$  4 mM;  $\alpha$ -ketoglutarate as indicated; 100  $\mu\text{g}$  enzyme protein.

Inset: Replot of intercept and slope against  $\alpha$ -ketoglutarate concentration.



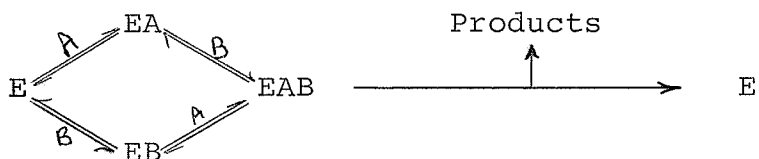
double reciprocal plots showing noncompetitive inhibition were obtained (Fig. 13). With glutamate at saturating level (200 mM) and  $\text{NAD}^+$  as the variable substrate ammonium showed uncompetitive inhibition (Fig. 14). When  $\text{NAD}^+$  was fixed (4 mM) and glutamate was the variable substrate with  $\text{NH}_4^+$  the inhibitor noncompetitive plots were again obtained (Fig. 15). Replots of slopes and intercepts against inhibitor concentration were linear and the  $K_i$  for  $\text{NH}_4^+$  was calculated.

With  $\alpha$ -ketoglutarate as product inhibitor and  $\text{NAD}^+$  as the variable substrate (fixed high glutamate) double reciprocal plots showed uncompetitive inhibition (Fig. 16). A replot of intercepts against  $\alpha$ -ketoglutarate concentration was linear. With glutamate as the variable substrate and  $\text{NAD}^+$  fixed (4 mM), however, using  $\alpha$ -ketoglutarate as the inhibitor, noncompetitive plots were obtained (Fig. 17). Again the replot was linear.

## II. B. A Kinetic Mechanism

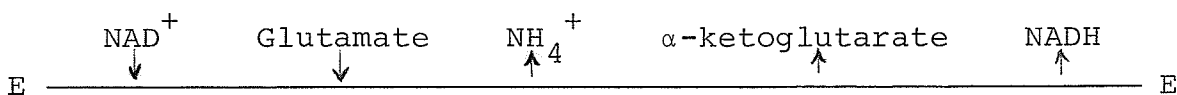
In the absence of AMP the complex non-linear double reciprocal plots make determination of a kinetic mechanism difficult. Since it was shown that  $\text{NAD}^+$  and glutamate can act as activators of the oxidative deamination reaction (Fig. 7 and 8), one cannot employ the simple single substrate-

single modifier reaction kinetic model to explain these findings. An alternate interpretation is that the kinetic mechanism may be Random. Diagrammatically the pattern would be:



where A and B represent  $\text{NAD}^+$  and glutamate respectively. On the basis of this concept one would expect that at saturating levels of one substrate, double reciprocal plots of rate against concentration of the other substrate should be linear. However, at very high levels of glutamate the plots are still nonlinear (Fig. 7). Thus, in the absence of AMP the kinetic analysis is ambiguous.

In the presence of AMP (saturating), however, reciprocal plots are linear. Thus, from the product inhibition studies a kinetic mechanism may be derived based on the suggestions of Cleland (6). Diagrammatically the proposed mechanism would be:



According to Cleland's terminology this would be an Ordered Binary-Ternary reaction in the oxidative deamination

direction in the presence of saturating AMP. A rate equation for the steady state may be derived by the method of King and Altman (20) using kinetic constants as defined by Cleland (6). The rate equation would be:

$$v = \frac{V_1 \left( AB - \frac{PQR}{K_{eq}} \right)}{K_{ia}K_b + K_bA + K_aB + AB + \frac{K_{ia}K_bK_qP}{K_pK_{iq}}}$$


---


$$\frac{K_{ia}K_bR}{K_{ir}} + \frac{K_bAP}{K_{ip}} + \frac{K_{ia}K_bK_rPQ}{K_pK_{iq}K_{ir}} + \frac{K_aBR}{K_{ir}} +$$


---


$$\frac{K_{ia}K_bQR}{K_{iq}K_{ir}} + \frac{K_{ia}K_bK_qPR}{K_pK_{iq}K_{ir}} + \frac{ABP}{K_{ip}} + \frac{K_{ia}K_bPQR}{K_pK_{iq}K_{ir}} +$$


---


$$\frac{K_rK_bAPQ}{K_pK_{iq}K_{ir}} + \frac{ABQ}{K_{iq}} + \frac{K_{ia}K_bBQR}{K_{ib}K_{iq}K_{ir}} + \frac{ABPQ}{K_{ip}K_{iq}}$$


---


$$\frac{K_{ia}K_bBPQR}{K_pK_{ib}K_{iq}K_{ir}}$$

where A = NAD<sup>+</sup>; B = glutamate; P = NH<sub>4</sub><sup>+</sup>; Q = α-ketoglutarate; and R = NADH; K<sub>a</sub>, K<sub>b</sub>, K<sub>p</sub>, K<sub>q</sub>, and K<sub>r</sub> are the respective Michaelis constants, and K<sub>ia</sub>, K<sub>ib</sub>, K<sub>ip</sub>, K<sub>iq</sub>, K<sub>ir</sub> are the

respective inhibition constants. When initial velocity studies are undertaken - products at zero concentration - this equation simplifies to:

$$V = \frac{V_1 AB}{K_{ia}K_b + K_bA + K_aB + AB}$$

In the specific case at point, analysis of product inhibition studies would be as follows: With P as inhibitor and A varied: P reacts with EQR while A reacts with E and thus they combine with different enzyme forms (Intercept change). If B is nonsaturating these forms, however, are reversibly connected by the sequence E-EA-EPQR- EQR and thus slope also varies giving non-competitive inhibition (Fig. 13). With B at saturating levels it is clear that the slope would remain constant (uncompetitive inhibition) (Fig. 14) as predicted by the equation:

$$\frac{1}{V} = \frac{K_a}{V} \left( 1 + \frac{K_{ia}K_b}{K_aB} \right) \left[ 1 + \frac{\frac{K_pK_{iq}}{K_aB} P}{\left( 1 + \frac{K_aB}{K_{ia}K_b} \right)} \right] \frac{1}{A}$$

$$+ \frac{1}{V} \left( 1 + \frac{K_b}{B} \right) \left[ 1 + \frac{P}{\frac{1 + K_b/B}{1/K_{ip} + K_b/K_{ip}B}} \right]$$

With P as inhibitor and B varied: P and B react with different enzyme forms (EQR and EA respectively) but these

forms are reversibly connected by the sequence  $EA \xrightleftharpoons{EPQR} EAB \xrightleftharpoons{EQR} EQR$  and thus noncompetitive inhibition results (Fig. 15)

$$\frac{1}{V} = \frac{K_b}{V} \left( 1 + \frac{K_{ia}}{A} \right) \left[ 1 + \frac{P}{\frac{K_p K_{iq}}{K_q}} \right] \frac{1}{B} + \frac{1}{V} \left( 1 + \frac{K_a}{A} \right)$$

$$\left[ 1 + \frac{P}{K_{ip} \left( 1 + \frac{K_a}{A} \right)} \right]$$

With Q as inhibitor and A varied: Q combines with ER while A combines with E. These two forms are not reversibly connected (P and R released at zero concentration). Therefore, uncompetitive inhibition results (Fig. 16).

$$\frac{1}{V} = \frac{K_a}{V} \left( 1 + \frac{K_{ia} K_b}{K_a B} \right) \frac{1}{A} + \frac{1}{V} \left( 1 + \frac{K_b}{B} \right) \left[ 1 + \frac{Q}{K_{iq} \left( 1 + \frac{K_b}{B} \right)} \right]$$

With Q as inhibitor and B varied: Q and B combine with different enzyme forms (ER and EA respectively). Thus, uncompetitive inhibition would be expected, since these forms are not reversibly connected. This type of inhibition is not achieved however (Fig. 17).

With R as inhibitor and A varied: A and R combine with the same enzyme form (E) and thus slope only is affected giving competitive inhibition (Fig. 12).

$$\frac{1}{V} = \frac{K_a}{V} \left( 1 + \frac{K_{ia} K_b}{K_a B} \right) \left( 1 + \frac{R}{K_{ir}} \right) \frac{1}{A} + \frac{1}{V} \left( 1 + \frac{K_b}{B} \right)$$

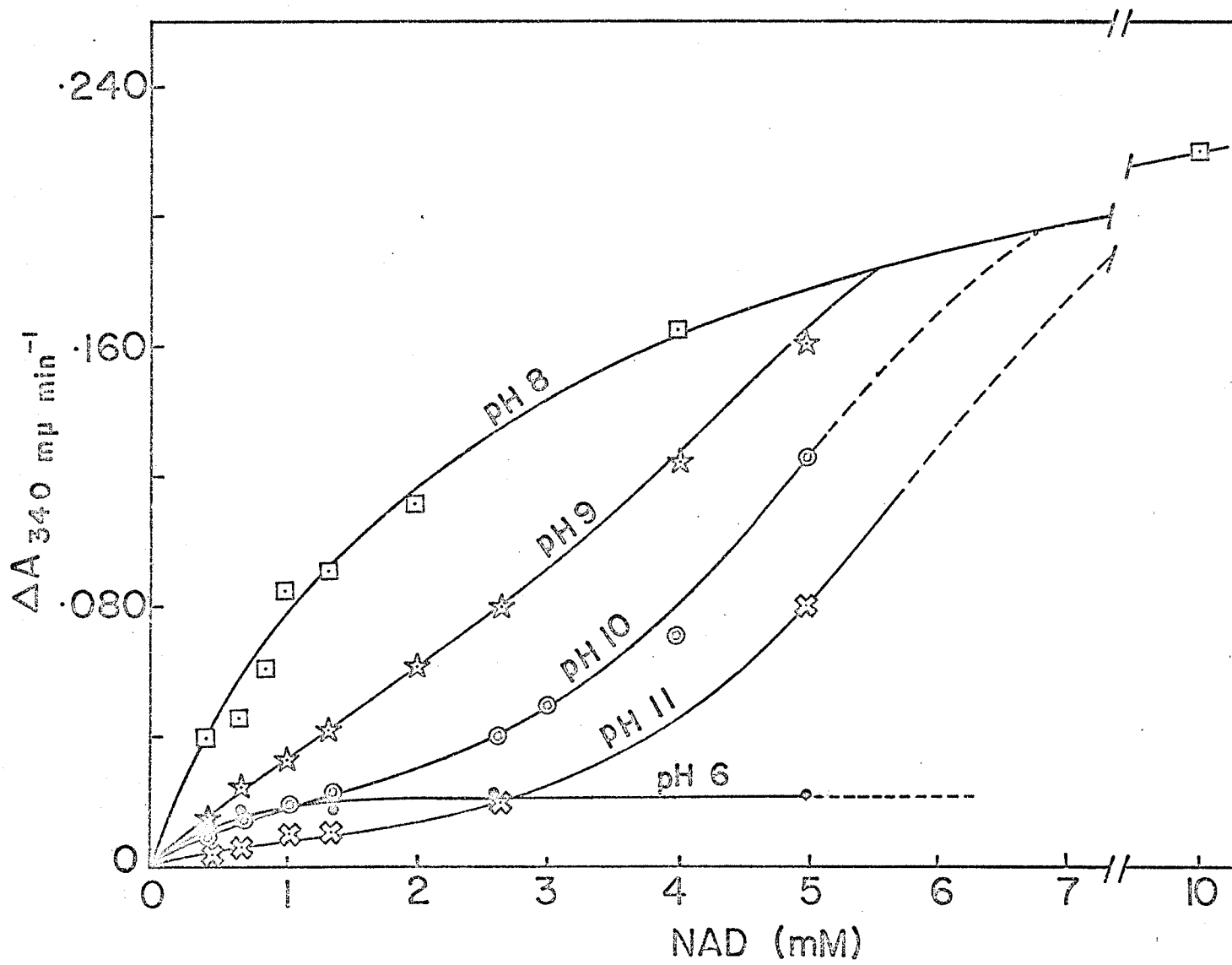
Thus it is evident that in all but one case (Q inhibitor, B varied) the experimental results are those predicted on the basis of the proposed mechanism. An explanation for the observed noncompetitive instead of uncompetitive inhibition has been advanced in the proposal of mixed dead-end and product inhibition.

### III. pH Effect on Kinetics

Preliminary studies to determine the pH optimum for the oxidative deamination of glutamate and the reductive amination of  $\alpha$ -ketoglutarate indicated a significant modifying influence of pH on enzyme activity, particularly in the presence of the activator, AMP. Similarly studies of pH influence on oxygen binding with haemoglobin (58) had produced the well-known Bohr effect. Thus, a study of the effect of pH on the reaction kinetics of glutamic dehydrogenase was undertaken.

The effect of pH on the oxidative deamination reaction in the absence of modifiers is shown in Fig. 18. Glutamate was fixed at a high level (66 mM) and  $\text{NAD}^+$  was the variable substrate. At pH 6, the enzymatic activity is low and there is no evidence of cooperativity. With increasing  $\text{NAD}^+$  levels, there is inhibition. The rate-concentration curve for pH 8

Figure 18. The effect of pH on the rate of the oxidative deamination of glutamate. Reaction mixtures contained 0.2 M Tris-chloride, pH as indicated; glutamate 66 mM;  $\text{NAD}^+$  as indicated; 50  $\mu\text{g}$  enzyme protein.



shows little evidence of cooperative interaction and activity is maximal (without modifiers). With increasing pH values plots became increasingly sigmoidal. Thus, it would seem that at pH 6, the enzyme is in some way 'desensitized' to activation by  $\text{NAD}^+$ .

#### IV. Interactions of pH and Purine Nucleotides

It was of interest to examine the nature of the enzyme response at different pH values in the presence of different concentrations of an activator (AMP). Apparently, high pH and low substrates tend to confer cooperative properties on the enzyme (Fig. 1 and 18). For the reductive amination reaction the results are shown in Fig. 19. The pH optimum was unchanged although the activating effect of AMP was particularly strong at alkaline pH's. It is obvious that, at pH 6, AMP has little effect on the reaction. This would indicate that the enzyme may have very different kinetic characteristics at this pH. Probably, a change in configuration has occurred and this has led to 'desensitization' of the enzyme toward its activator. At the pH optimum, however, activation by AMP is 2.5 fold. At high pH values AMP activation was more pronounced (At pH 9 the activation was 4-fold and at pH 10.5-fold).

Figure 19. Interactions between pH and AMP at fixed concentrations of  $\alpha$ -ketoglutarate (5 mM) and NADH (.166 mM) and  $\text{NH}_4^+$  (250 mM). Reaction mixtures contained 0.2 M Tris-chloride, pH range indicated; levels of AMP as indicated; 100 $\mu$ g enzyme protein.

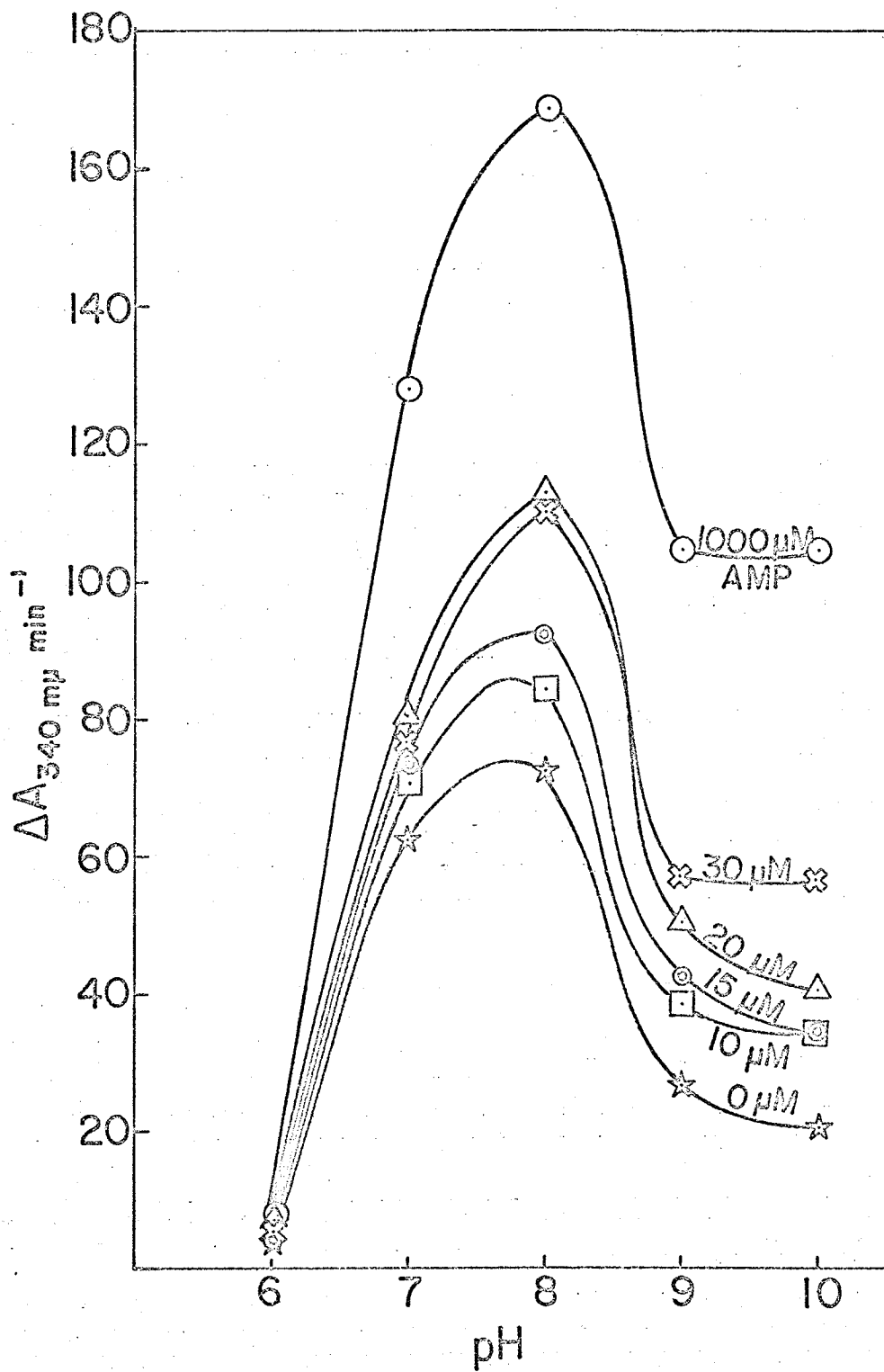
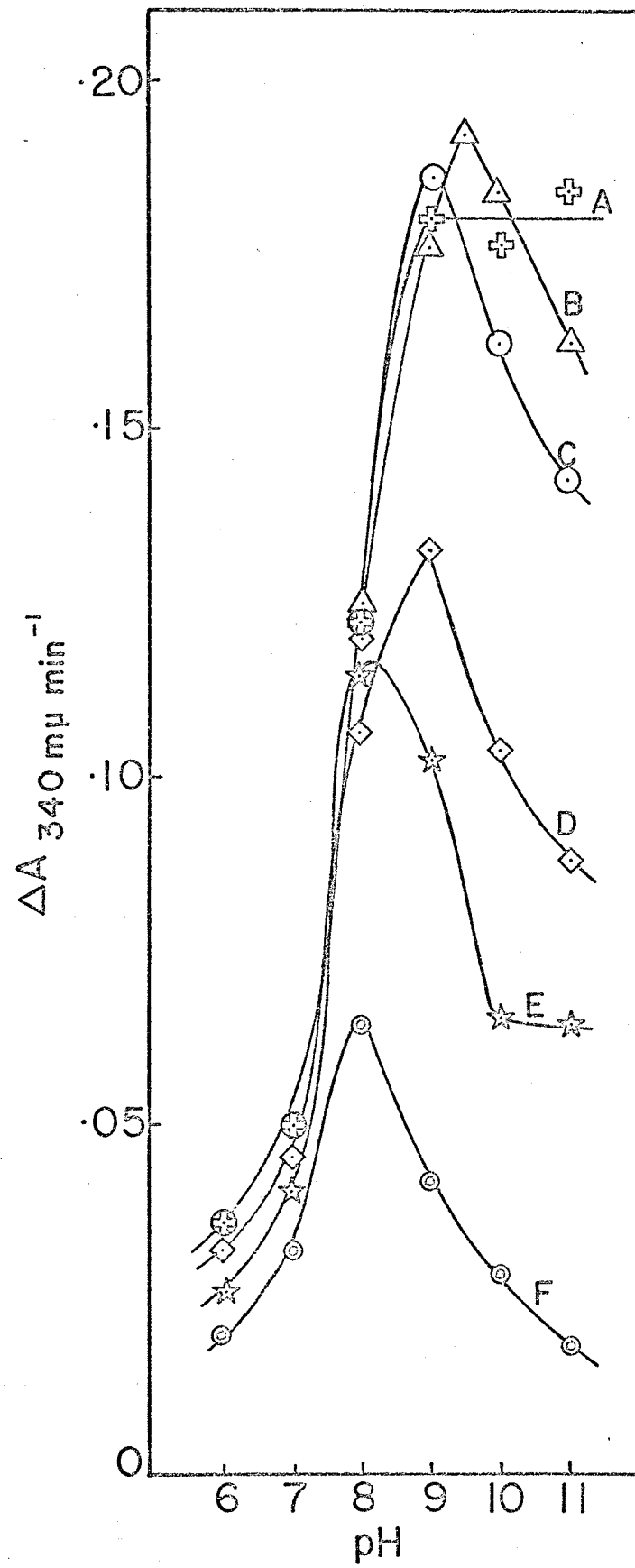


Figure 20. Interactions between pH and AMP at fixed high concentrations of  $\text{NAD}^+$  (2.66 mM) and glutamate (33.3 mM). Reaction mixtures contained 0.2 M Tris-chloride, pH as indicated; several levels of AMP (A, 1 mM; B, 0.1 mM; C, 0.05 mM; D, 0.01 mM; E, 0.005 mM; and F, 0 mM); 12  $\mu\text{g}$  enzyme protein.



When the oxidative deamination reaction was studied the situation appeared more complex (Fig. 20). Again at pH 6 AMP caused very little activation of the reaction. At pH 11, however, activation was 8-fold. The most significant difference here, however, is that with increasing levels of AMP not only does activation increase, but also the pH optimum shifts from a value of 8 in the absence of AMP to a value approaching 10 at saturating AMP levels. It is implicit in these and other data presented previously that protons themselves may be acting as important regulatory ligands. This effect, not observed in the reductive amination reaction, leads to interesting implications with regard to a physiological control mechanism. This point will become increasingly apparent in later sections.

## V. Zone Sedimentation Analysis by Sucrose Density Gradients

### A. Molecular Weight Determination

Sucrose density gradient determination of the molecular weight of NAD-specific glutamic dehydrogenase was carried out as described in Materials and Methods. Pig heart malate dehydrogenase (Boehringer) was used as an internal standard in molecular weight determination.

Assuming a molecular weight of 40,000 for the malate dehydrogenase, the glutamic dehydrogenase was estimated to have an average molecular weight of  $200,000 \pm 20,000$ .

B. Influence of Protons and Modifiers on the Sedimentation Behaviour of Blastocladiella emersonii glutamic dehydrogenase.

Attempts were made to study the effects of pH and various effectors on the enzyme from a physical standpoint in order to support the kinetic observations (Table IV). In previous studies (30) it was observed that the enzyme was inactivated at alkaline pH's when run in sucrose density gradients provided effectors or substrates were absent. To relate the kinetic changes observed (Fig. 18) to this inactivation and probable association-dissociation of the enzyme, sucrose density gradient centrifugations were conducted over a wide range of pH values in the presence and absence of a diversity of ligands (Fig. 21).

In the absence of effectors the pH effect was considerable. At pH values of 6 and 8 about 50 per cent of the initial activity was lost. There was no discernible change in the molecular weight of the enzyme. The inactivation of the enzyme seen at high pH values could be due to a partial dissociation of the enzyme.

Figure 21. Zone centrifugation of Blastocladiella glutamic dehydrogenase in sucrose density gradients.

Gradients contained 120  $\mu$ g enzyme protein.

(a) Run 35,000 r.p.m. for 18 hours; (b)-(f)

30,000 r.p.m. for 20 hours. Additions and pH as indicated.

Assay mixture contained 50  $\mu$ l gradient fraction;

3.33 mM  $\alpha$ -ketoglutarate; 0.166 mM NADH; 500 mM  $\text{NH}_4^+$ ; 1 mM AMP; and 0.2 M Tris-chloride buffer, pH 7.

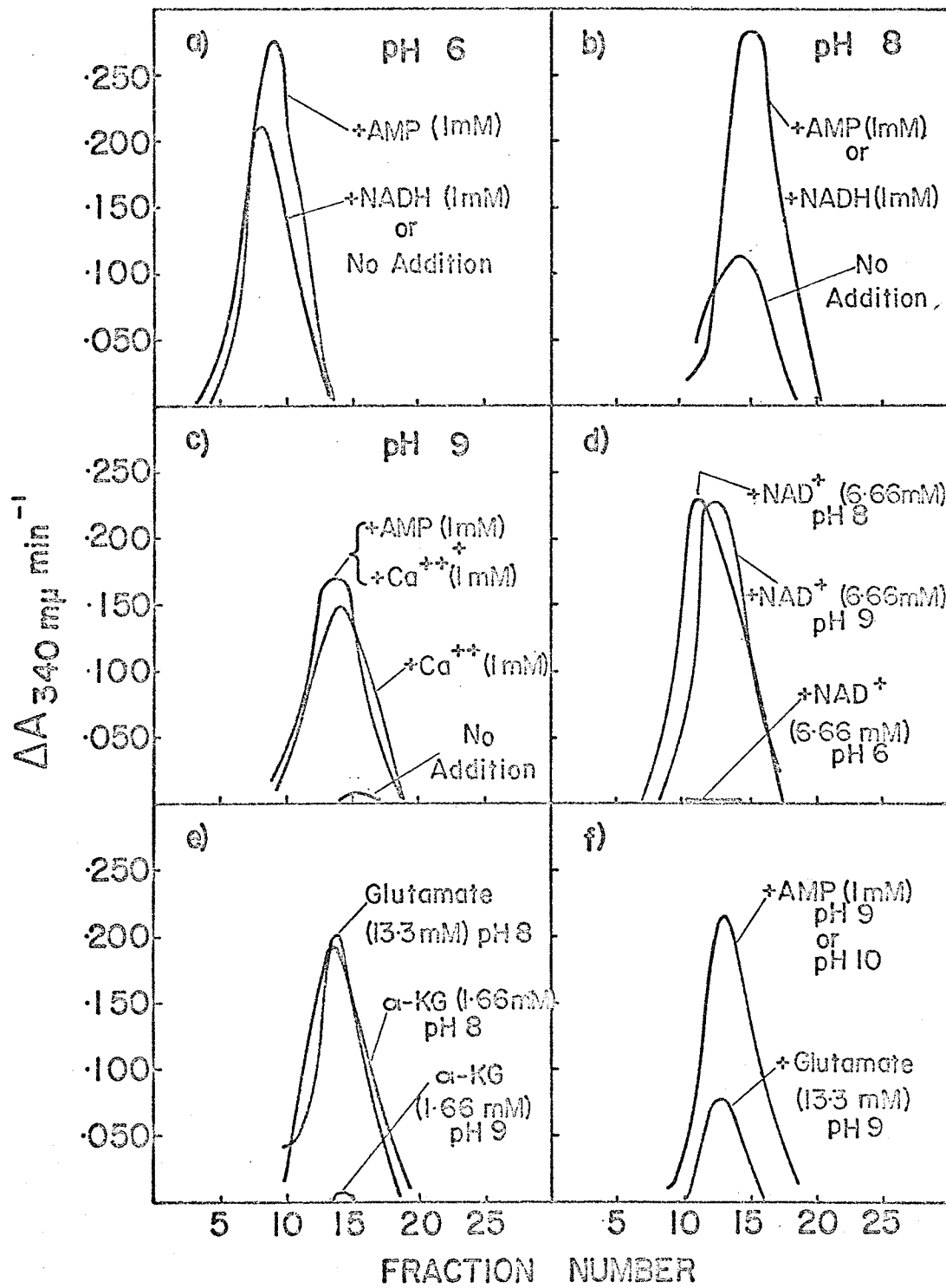


Table IV

pH	Activity Before Centrifuge per 100	No Addition	+AMP	+Ca <sup>++a</sup> AMP	+NAD +NADH <sup>b</sup>	+ glutamate + $\alpha$ -Kg <sup>c</sup>	% Recovery	Activity Peak
6	1340	753					56	8
	1340		968				72	9
	1340				763 <sup>b</sup>		57	8
	920						0	-
8	960	490					51	14
	960		1130				100	15
	960				998 <sup>b</sup>		100	15
	920				985		100	11
	920					857	93	14
	920					815 <sup>c</sup>	89	14
9	920						0	-
	920			690 <sup>a</sup>			75	14
	920			760			83	13-14
	920				865		94	12
	920						0	-
	840					190	23	13
	840			895			100	13
10	840		855				100	13

Upon addition of effectors several differences became apparent in the activity patterns. At pH 8 and higher, the full activity of the enzyme was recovered in the presence of AMP (Table IV).

Pyridine nucleotides failed to enhance recovery at pH 6. The presence of  $\text{NAD}^+$  (6.66 mM) in the gradient completely inactivated the enzyme although NADH was without effect. At alkaline pH's both  $\text{NAD}^+$  and NADH protected the enzyme and near full recovery was obtained even at unfavourable pH levels (pH 9 and above).

As well as pyridine and purine nucleotides, other substrates were added to the gradients. At pH 8,  $\alpha$ -ketoglutarate (1.66 mM) enhanced recovery to a certain extent (89% compared to 51% in the absence of substrate). At pH 9, however,  $\alpha$ -ketoglutarate was totally ineffective in protecting the enzyme from inactivation. Glutamate (13.33 mM) also showed some enhancement of recovery at pH 8 (Table IV). At pH 9, however, only 20 per cent of the activity was recovered. This would seem to indicate that these substrates probably do not bind very well to the free enzyme at high pH's and therefore cannot protect it against ionization by hydroxyl ions.

Kinetic studies to be discussed later (31) indicated the involvement of cations, specifically  $\text{Ca}^{++}$ , in the

enzyme reaction. Therefore, in order to determine if  $\text{Ca}^{++}$  did in fact bind the free enzyme, density gradient analysis was made. It was found that  $\text{Ca}^{++}$  (1 mM) in the gradient preserved 73 per cent of the initial activity at the unfavourable pH value of 9. Thus, one may conclude that  $\text{Ca}^{++}$  binds the free enzyme form. When both  $\text{Ca}^{++}$  and AMP were present in the gradient, an additional ten per cent of the activity was recovered. Although perhaps surprising, it is obvious that  $\text{Ca}^{++}$  is nearly as effective as AMP and  $\text{NAD}^+$  in protecting the enzyme from inactivation at alkaline pH. This effect will be discussed more fully later in relation to the physiological implications.

#### VI. Influence of Cations on Substrate-substrate Interactions

In the report of LeJohn (31) it has been shown that various cations exert an influence on the substrate-substrate interactions of the glutamic dehydrogenase reaction. In order to facilitate a discussion of the probable mechanism of the enzyme in vivo, a brief account of those results becomes necessary.

In studying the reductive amination reaction it was found that certain cations activated the reaction while others inhibited it (Table V).  $\text{Ca}^{++}$  and  $\text{Mn}^{++}$  were activators. Activation by  $\text{Mg}^{++}$  was very slight, while  $\text{Zn}^{++}$ ,  $\text{Cu}^{++}$ , and  $\text{Co}^{++}$  were, in varying degrees, inhibitory.

Table V. The reaction system contained NADH 0.166 mM;  $\alpha$ -ketoglutarate 1.66 mM;  $\text{NH}_4^+$  500 mM; 0.2 M Tris-chloride buffer, pH 7; 5  $\mu\text{g}$  enzyme protein. All solutions were made up to pH 7 just before use.

Table V

The Effect of Cations on the Reductive Amination of  $\alpha$ -ketoglutarate by Blastocladiella Glutamic Dehydrogenase.

Addition	Concentration (mM)	$A_{340} \text{ m}\mu \text{ min.}^{-1}$	Inhibition (%)	Activation (%)
None	-	0.040	-	-
AMP	1	0.088	-	120
Ca <sup>++</sup>	3.33	0.075	-	85
Mn <sup>++</sup>	3.33	0.065	-	65
Mg <sup>++</sup>	3.33	0.044	-	10
Zn <sup>++</sup>	3.33	0.008	80	-
Cu <sup>++</sup>	3.33	0.000	100	-
Co <sup>++</sup>	3.33	0.034	12	-

In Fig. 22 the effect of  $\text{Ca}^{++}$  on the oxidative deamination of glutamate is shown. The inset shows the reaction in the absence of effector and in the presence of the positive effector (AMP or ADP) for comparison. Increasing concentrations of  $\text{Ca}^{++}$  had a significant inhibitory effect on the reaction. High concentrations of  $\text{NAD}^+$  seemed incapable of reducing  $\text{Ca}^{++}$  inhibition. Thus, the response may be non-cooperative.

Double reciprocal plots of Fig. 23 and 24 illustrate the effect of various modifiers, including  $\text{Ca}^{++}$ , on the reductive amination reaction.

With  $\alpha$ -ketoglutarate as the variable substrate (Fig. 23) it is immediately seen that  $\text{Ca}^{++}$  activated the reaction almost to the same extent as AMP did. Also clear is the critical level for substrate inhibition. A slight increase in substrate tolerance is seen with  $\text{Ca}^{++}$  and AMP. The inhibition by ATP illustrates the opposite effect, i.e., a decrease in concentration of substrate inhibiting the reaction.

With NADH as the variable substrate the plots in Fig. 24 are obtained. Again activation by  $\text{Ca}^{++}$  approaches that by AMP. In this plot the shift in inhibitory level of substrate is more evident.  $\text{Ca}^{++}$  activated the reaction greatly at low NADH concentrations. Difficulties arise

Figure 22. Rate-concentration representation of the effect of  $\text{Ca}^{++}$  on the oxidative deamination of glutamate. Reaction system contained 16.66 mM glutamate; 4 mM  $\text{NAD}^+$ ; 18  $\mu\text{g}$  enzyme protein, 0.15 M Tris-chloride buffer, pH 9, and  $\text{Ca}^{++}$  as indicated.

Inset. Rate-concentration profile of activation by AMP or ADP (100  $\mu\text{M}$  level) in the system described above.

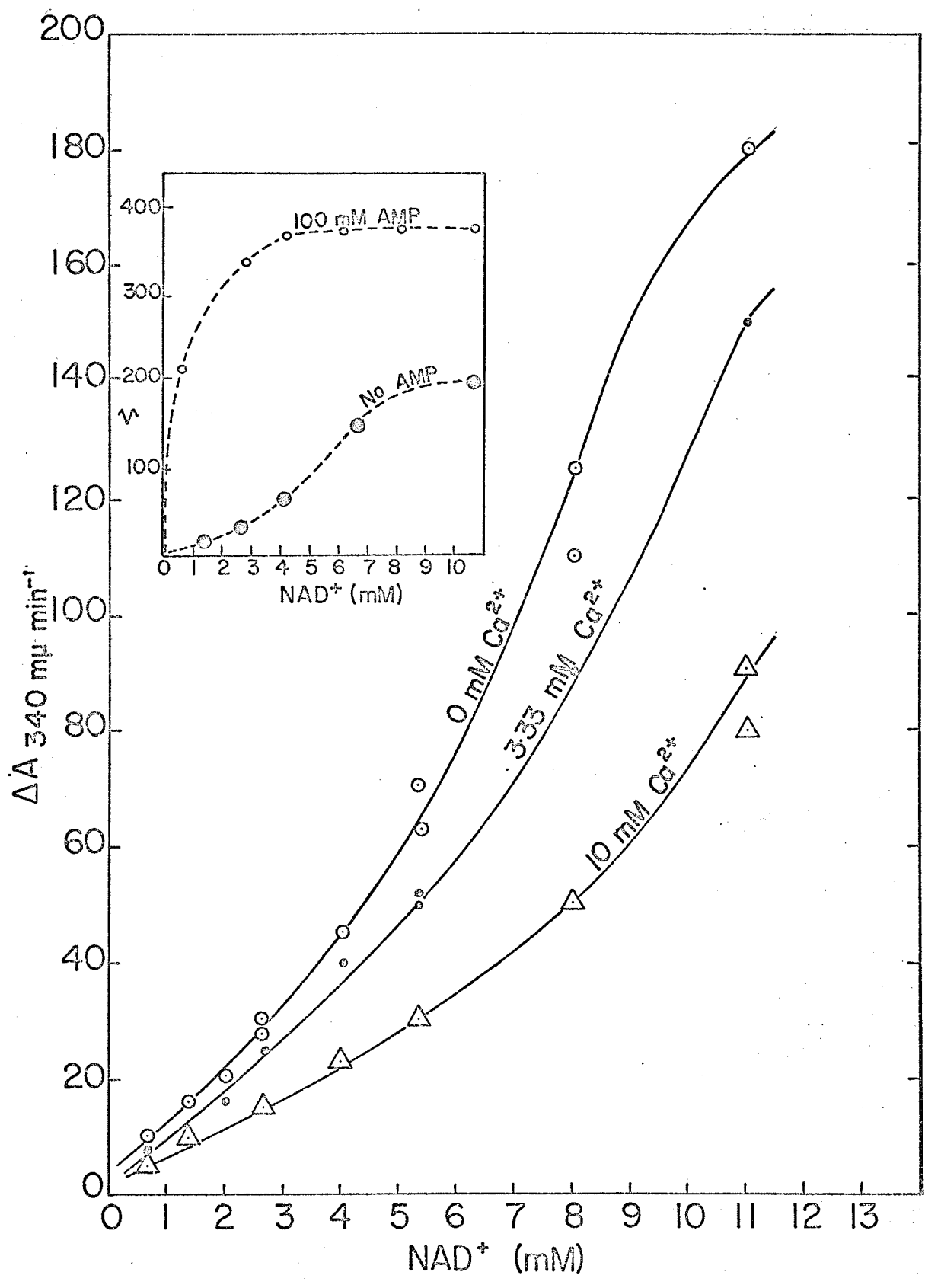


Figure 23. Lineweaver-Burk representation of the effect of  $\text{Ca}^{++}$ , AMP, ADP, and ATP on the reductive amination of  $\alpha$ -ketoglutarate.  $\alpha$ -Ketoglutarate was the varied substrate at a fixed concentration of NADH (0.166 mM);  $\text{NH}_4^+$  (500 mM); 5  $\mu\text{g}$  enzyme protein; 0.15 M Tris-chloride buffer, pH 7; additions as indicated.

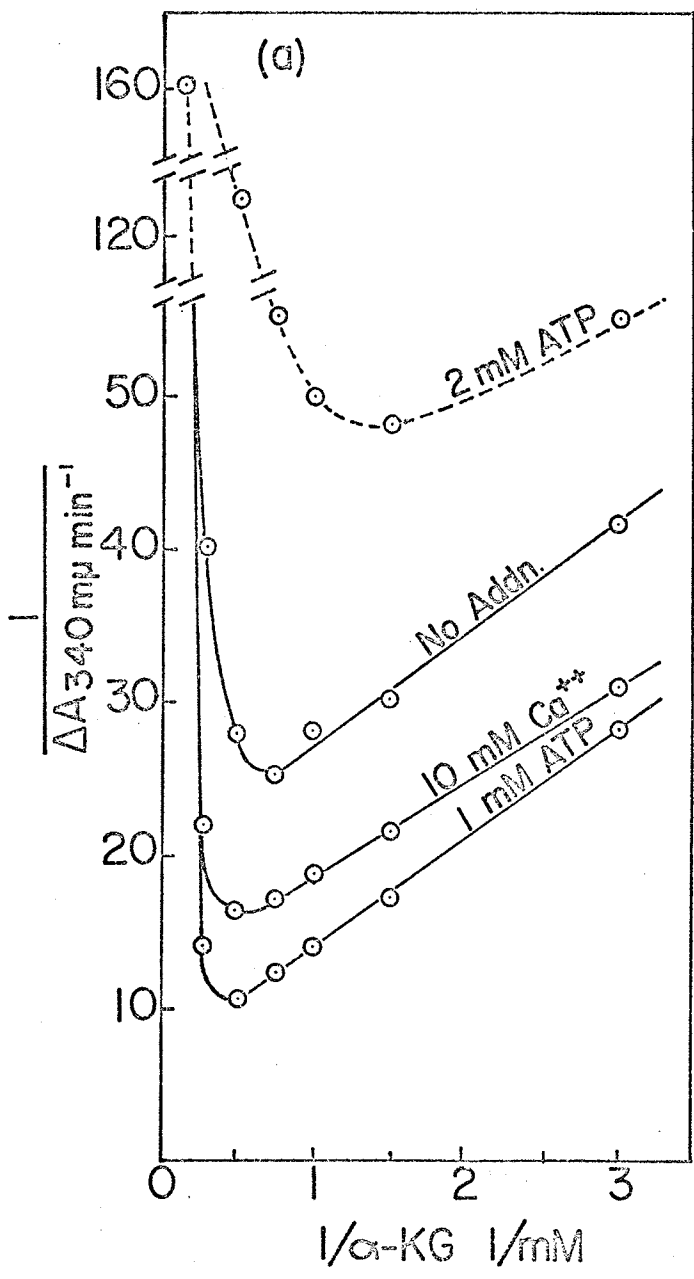
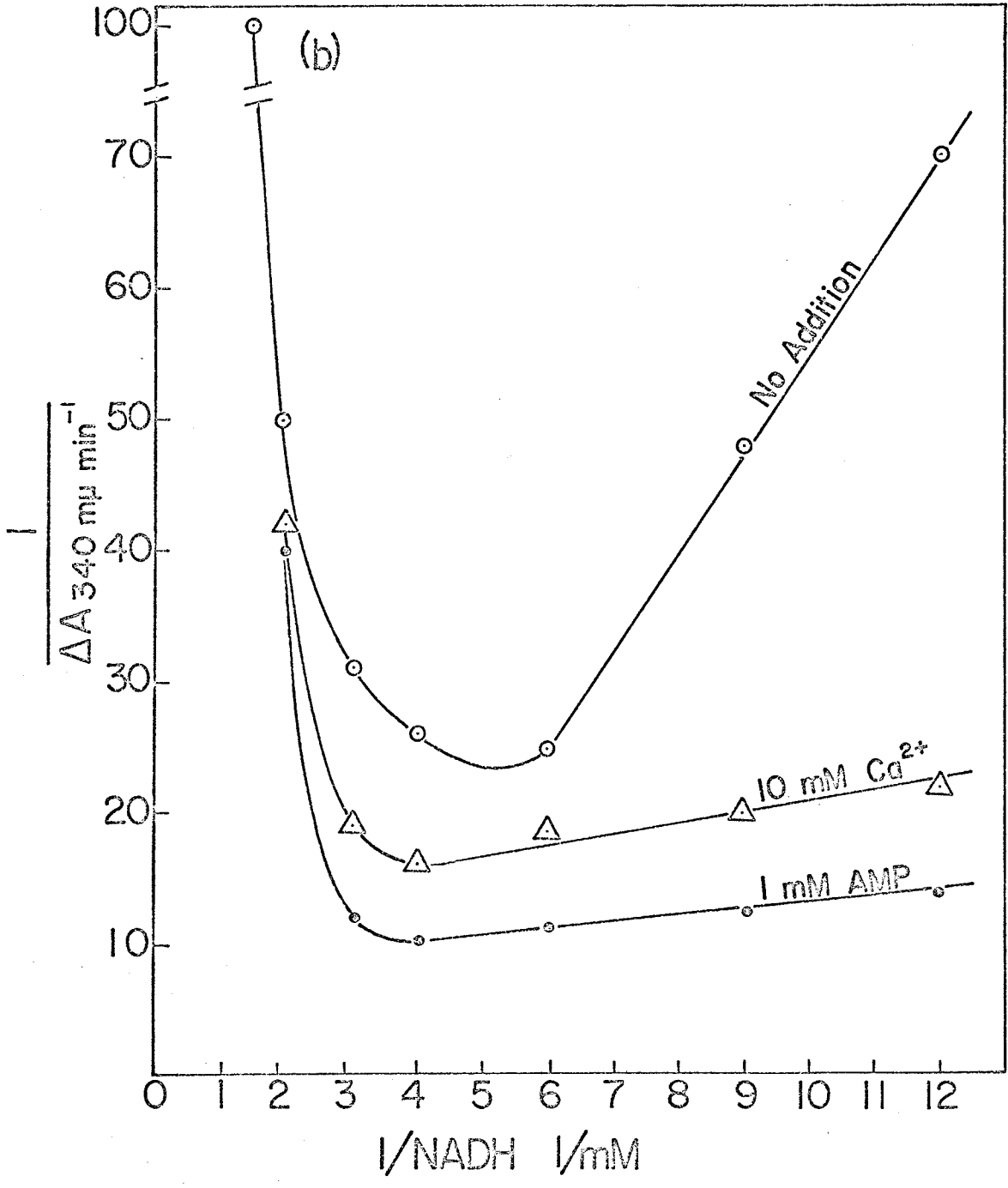


Figure 24. Lineweaver-Burk representation of the effect of  $\text{Ca}^{++}$  and AMP on the reductive amination of  $\alpha$ -ketoglutarate. NADH was the varied substrate at a fixed concentration of  $\alpha$ -ketoglutarate (1.66 mM);  $\text{NH}_4^+$  (500 mM); 5  $\mu\text{g}$  enzyme protein; 0.15 M Tris-chloride buffer, pH 7;  $\text{Ca}^{++}$  and AMP as indicated.



when attempts are made to analyse these plots due to the sharply defined substrate inhibition levels. One thing is clear and that is that  $\text{Ca}^{++}$  and AMP are unable to overcome substrate inhibition although they both can activate the reductive amination reaction.

#### VII. Dependence of Cationic Effects on pH

LeJohn (31) has also been able to demonstrate a subtle dependence of the cationic effect on pH. The results of this study are summarized in Table VI. In Table VI(a) the interactions for the reductive amination reaction are shown. It is evident that at pH 6  $\text{Ca}^{++}$  and  $\text{Mn}^{++}$  have no activating effects. This is particularly interesting because of a similar pH response when purine and pyridine nucleotides interact with the enzyme at pH 6. At higher pH values activation by  $\text{Ca}^{++}$  is enhanced. The regulatory aspect of these cationic and proton effects will be dealt with in detail in the "Discussion".

When the oxidative deamination reaction was studied it was found that higher pH values favoured  $\text{Ca}^{++}$  inhibition of the reaction (Table VI). This logically fits an interacting control pattern of regulation of the reaction by pH and cations.

Table VI a) The reaction system is an outlined in Table V  
15  $\mu\text{g}$  enzyme protein was used and buffers set at  
desired pH.

b) The reaction system contained  $\text{NAD}^+$ , 4 mM;  
glutamate, 16.66 mM; 40  $\mu\text{g}$  enzyme protein and  
buffers at the specified pH.

Table VI

The Effect of  $\text{Ca}^{++}$  and  $\text{Mn}^{++}$  on (a) The Reductive Amination of  $\alpha$ -Ketoglutarate; (b) the Oxidative deamination of Glutamate by Blastocladiella Glutamic Dehydrogenase.

Addition	Reaction Rate* (pH)			
	(6)	(7)	(8)	(9)
(a)				
None	0.006	0.125	0.054	0.015
10 mM $\text{Ca}^{++}$	0.010	0.322	0.190	0.045
10 mM $\text{Mn}^{++}$	0.005	0.264	0.188	-
% Activation by $\text{Ca}^{++}$	0	255	350	300
% Activation by $\text{Mn}^{++}$	0	200	350	-
(b)				
None	0.038	0.140	0.084	0.068
10 mM $\text{Ca}^{++}$	0.040	0.142	0.060	0.028
% Inhibition by $\text{Ca}^{++}$	0	0	30	60

\*Reaction Rate =  $\Delta A_{340 \text{ m}\mu} \text{min}^{-1}$

### VIII. Mitochondrial Work

Attempts were made to isolate intact mitochondria in order to substantiate the proposal that this glutamic dehydrogenase is present in the mitochondria (probably on the outer membrane). When mitochondria were isolated it was found that the specific activity of the enzyme in mitochondrial protein was very high compared to that of cytoplasmic protein (Table VII). Thus, one may tentatively conclude that the enzyme is associated with the mitochondria and that presumably it is located in a position from which it may be easily detached in mitochondrial preparation, ie, the outer membrane.

### IX. Unidirectional Inhibition by Metabolites

As a further development of effector studies on the glutamic dehydrogenase reaction, LeJohn (32) reported the influence of various citric acid cycle intermediates on the reaction. Since this work further facilitates discussion of a physiological regulation pattern, the results will be summarized here.

It was found that of the compounds tested only ATP exerted a noticeable effect on the reductive amination of  $\alpha$ -ketoglutarate (Table VIII). However, in the oxidative deamination of glutamate, several compounds exerted strong

Table VII

Mitochondrial Data		
	Pellet	Supernatant
Total Volume (ml)	0.6	12.0
Total Activity	500 units	24,000 units
Total Protein	1.05 mg	84 mg
Specific Activity	476	285.7
% Activity	62.5	37.5

Table VIII. Effect of metabolites and nonmetabolites on the reductive amination activity of Blastocladiella glutamic dehydrogenase. Reaction system contained: 20  $\mu$ g enzyme protein; 6.66 mM  $\alpha$ -ketoglutarate; 66  $\mu$ M NADH; 1 mM AMP (where indicated); 500 mM  $\text{NH}_4^+$ ; and 150 mM Tris-chloride buffer pH 7.8.

<sup>a</sup> Ratio of velocities where  $v_0$  and  $v_1$  represent reaction rates in the absence and in the presence of AMP, respectively;  $v$  and  $v_2$  represent the reaction rates in the absence and in the presence of AMP, respectively with several different metabolites and nonmetabolites.

Table VIII

Addition	Conc <sup>n</sup> (mM)	v/v <sub>0</sub> <sup>a</sup> (-AMP)	v <sub>2</sub> /v <sub>1</sub> <sup>a</sup> (+AMP)
None		1.00	1.00
Citrate	33.33	1.31	1.35
ATP	1.00	0.00	0.94
EDTA	10.00	1.25	1.27
Fructose-1,6-di-P	33.33	1.00	1.15
8-Hydroxyquinoline	1.00	1.08	1.06
Sodium diethyl- dithiocarbamate	10.00	1.06	1.08
Isocitrate	33.33	0.80	0.85
Succinate	33.33	0.95	1.26
Fumarate	33.33	0.91	0.92
P-enolpyruvate	33.33	1.00	1.35
Oxaloacetate	33.33	1.02	1.13
Glucose-6-P	33.33	0.98	1.19
Acetyl CoA	0.166	1.00	1.14

Table IX. Effect of metabolites and nonmetabolites on the oxidative deamination of glutamate. The reaction system contained: 40  $\mu$ g enzyme protein; 13.33 mM glutamate; 4 mM  $\text{NAD}^+$ ; 1 mM AMP (where indicated); and 150 mM Tris-chloride buffer, pH 9.

<sup>a</sup>See Table VIII for definitions.

Table IX

Addition	Conc <sup>n</sup> (mM)	$v/v_0^a$ (-AMP)	$v_2/v_1^a$ (+AMP)
None		1.00	1.00
EDTA	0.066	0.00	0.99
Sodium diethyl- dithiocarbamate	3.33	0.50	1.00
8-Hydroxyquinoline	1.00	0.30	0.98
ATP	1.00	0.00	0.98
Citrate	3.33	0.05	1.00
Isocitrate	3.33	0.50	1.00
Fructose-1,6-di-P	3.33	0.50	1.00
$\alpha$ -Ketoglutarate	3.33	0.50	0.59
Fumarate	3.33	0.55	0.97
Succinate	3.33	0.65	1.01
Glucose-6-P	3.33	0.83	1.00
P-enolpyruvate	3.33	0.88	1.02
Oxaloacetate	3.33	0.88	0.99
Acetyl CoA	0.166	0.98	1.00

inhibitory effects (Table IX). Citrate, isocitrate, fumarate, succinate, fructose 1,6-diphosphate, and  $\alpha$ -ketoglutarate, as well as ATP, inhibited the reaction. The non-metabolite EDTA also completely inhibited the reaction at 60  $\mu$ M levels while concentrations as high as 10 mM EDTA had no effect on the reductive amination reaction. This unidirectional inhibition is surprising when one considers the 'microscopic reversibility' of the reaction. Nevertheless, it affords a useful regulation device in terms of physiological control.

Citrate was the most potent metabolite that inhibits the reaction. At very low concentrations citrate drastically inhibits glutamate breakdown. In the presence of AMP (0.1 mM), however, citrate does not display a sigmoid response but does lower the net reaction velocity. Thus, AMP effectively relieves citrate inhibition. In a Lineweaver-Burk representation with AMP as the variable substrate, citrate as inhibitor, an uncompetitive inhibition relationship was obtained. This would indicate that citrate and AMP do not bind to the same regulatory site. Citrate and glutamate (variable substrate) showed non-competitive inhibition. At low glutamate levels and high citrate concentration, the double reciprocal plots deviate markedly from a linear pattern.

The influence of pH on the inhibition pattern was studied so as to eliminate the problem of pH effect on the inhibitory ligand dissociation constant. At low pH citrate showed little inhibition. (No inhibition was evident at pH 6.) With increasing pH, however, citrate inhibition became pronounced. Using the same pH range the metabolites were found to exert no adverse effects on the reductive amination reaction.

Because the metabolites and non-metabolites (ATP, EDTA) exerting such strong inhibitory effects on the oxidative deamination reaction are all chelating agents in one form or another, other non-physiological chelating agents were tried and found to exert a similar inhibition on the reaction. In most cases this inhibition, like metabolite inhibition, could be relieved by divalent cations and AMP. The physiological implications of a probable chelation mechanism with regard to regulation will be developed in the "Discussion".

## DISCUSSION

SECTION A. A Molecular Mechanism

Based on the general kinetic observations and the sucrose density gradient studies a molecular model of the enzyme is tentatively formulated. Considering the molecular weight estimation of about 200,000 for glutamic dehydrogenase from Blastocladiella emersonii and assuming a basic subunit size of 50,000 molecular weight (based on the estimation for the bovine liver enzyme by Frieden (11) ), four subunits may be present. The tenuous evaluation of four ATP (hence AMP) interacting sites (Fig. 6) would tend to support this idea.

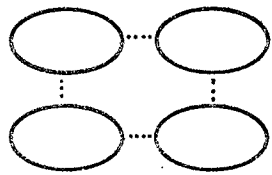
Koshland's concept of sequential binding (23, 24) and subunit interaction (25) can be invoked to explain the observed loss of activity in the gradients without perceptible change in molecular weight, i.e., the lack of substrate or effector does not afford the protection necessary to conserve the active site(s) in the correct configuration under hydrodynamic stress.

Although the apparent absence of a change in molecular weight would seem to negate the possibility of dissociation, it would seem likely that a weakening or disorientation of interprotomer bonds, as a consequence of hydrostatic pressures developed during centrifugation, would be the most plausible explanation for the activity loss.

Figure 25. An allosteric model for Blastocladiella glutamate dehydrogenase.

'A' represents a partially dissociated tetramer; 'B' represents the typical 'T' state of Monod et al ( 43); and 'C' the 'R' state. The transition 'A'  $\longrightarrow$  'B'  $\longrightarrow$  'D' is affected by the ionic environment. The 'D' state, because of its inactivity, has been deliberately ignored in the discussion.

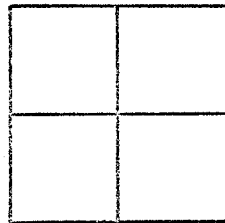
"loosely associated"



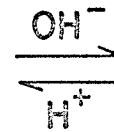
(A)



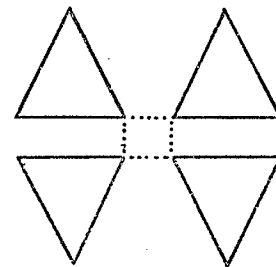
"tight"



(B)



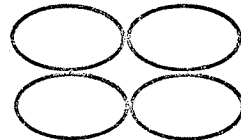
"inactive"



(D)

$\alpha$ -KG, ATP, NADH  $\updownarrow$  NAD, AMP, GLUTAMATE

"relaxed"



(C)

Thus, despite the applicability of Koshland's concept here and to several other observations, the model presented is based largely on the concept of Monod et al (43). On this basis, it is presumed that the tetramer consists of isologous association of monomers.

A preliminary model is presented in Fig. 25. On the basis of this model many phenomena observed in initial reaction rate studies may be explained. The precepts of the model are as follows:

a) The isolated protein is primarily in the B state which is in equilibrium with C, and likely A. The A-B equilibrium may be regulated by some innate property of protein-protein interaction which confers a specific symmetry conformation to the oligomer.

b) State A consists of a loosely associated, unstable tetramer which can dissociate to form inactive monomers. Given the proper ionic environment these monomers can realign, by virtue of symmetry and specificity of association, to form B even at high protein dilutions.

c) Although state A is active it is 'desensitized' to nucleotide activation. This form would predominate at pH 6 (Fig. 18) where cooperativity is not evident.

d) At high pH (above 9) forms B and C predominate and should show cooperativity between substrates and modifiers

(Fig. 18 and 20). Under these conditions nucleotide activation is pronounced with concomitant enhancement of sigmoidicity in saturation curves.

e) Forms A and C possess similar high affinities for certain ligands (substrates). Because of desensitization, however, nucleotide activation is not evident for A. The B form has an extremely low affinity for these same substrates.

f) The shape of the saturation profile would then indicate the statistical distribution of various enzyme forms at a given ligand concentration and ionic environment. In the absence of modifiers at low pH and low substrate levels the equilibrium would rapidly shift to A because of dilution in kinetic assays. Thus, a hyperbolic curve would result (Fig. 18). At increased pH values, however, or in the presence of activators, equilibrium would favour B which would then describe a sigmoid pattern in its transition to the highly reactive C even at low protein and substrate concentrations (Fig. 4 and 18).

One prediction that nucleotides should 'freeze' the enzyme in a particular conformation that is now stable against inactivation by pH has been supported in density gradient studies (Results V).  $\text{NAD}^+$  is an exception to this prediction in that it causes inactivation of the enzyme at pH 6 in density gradients.

Subsequent studies on unidirectional inhibition by diverse metabolites and cations (31, 32), however, required modification of this concept.

The fact that inhibition by chelation effects are observed only in glutamate breakdown leads to two possibilities. The first would implicate a loosely bound metal ion as a regulatory molecule that may be essential for the reaction process. This proposal could be explained on the basis of Koshland's flexible active site hypothesis ('induced fit') (23) whereby substrate binding induces a conformational change (or possibly merely a charge redistribution) in the protein. Because of different conformations induced by the various substrate ligands in the two directions of the reaction, this metal ion may either be exposed or buried - and hence inaccessible - depending on the substrates which are bound to the enzyme. In this instance binding of  $\text{NAD}^+$  and/or glutamate would cause exposure of the ion to chelating agents, thereby inhibiting formation and/or release of products by steric hindrance or conformational change. The second possibility implies a more generalized mechanism of unidirectional inhibition. This alternative will be developed later.

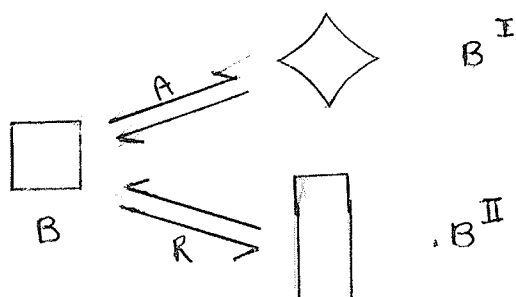
In the presence of AMP at saturating levels all enzyme protein exists in the C form. Citrate has no inhibitory effect under these conditions. Therefore, AMP

must alter the binding property of the protein toward citrate, thus preventing chelation.

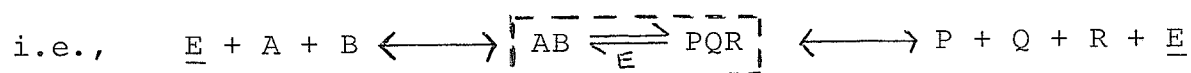
$\text{Ca}^{++}$  effects on the oxidative deamination reaction may be explained on the basis of two glutamate sites. At low levels of glutamate  $\text{Ca}^{++}$  inhibits the reaction. At high glutamate levels, however,  $\text{Ca}^{++}$  overcomes glutamate inhibition. This may be explained by the fact that the second glutamate site - the inhibitor site - would be filled by  $\text{Ca}^{++}$  and thus prevent inhibition. (At low glutamate levels  $\text{Ca}^{++}$  could compete for the active site thus causing inhibition.)

When one attempts to extend this model to the reversible reaction, complications arise. In order to explain the unidirectionality of inhibition one must assume that different enzyme forms function in opposite directions of the reaction. From product inhibition studies  $\text{NAD}^+$  and  $\text{NADH}$  seem to bind the same enzyme form (Fig. 12), presumably the free enzyme (Results V). Also mentioned previously was the assumption that the isolated enzyme protein exists largely in the B state. Based on stereochemical considerations one may propose differential conformational changes upon binding of these two pyridine nucleotides. When  $\text{NAD}^+$  binds to the protein, it is believed to tend to lie flat on the protein surface while  $\text{NADH}$  tends to assume a vertical position relative to the protein surface (21). Also, in

general, reduced coenzymes are more tightly bound to protein than are oxidized forms (37). Thus, it is not unlikely that the differential effect on conformation of a protomer by binding of one rather than the other could be extreme. As an example:



Kinetically defined  $B^I$  represents EA while  $B^{II}$  represents ER (A and R being  $NAD^+$  and NADH respectively). Therefore, although both A and R combine with the same enzyme form, E (the free enzyme), EA and ER complexes are significantly different. Therefore, subsequent binding of glutamate (B) to EA or  $\alpha$ -ketoglutarate (Q) and  $NH_4^+$  (P) or ER must sufficiently realign the protein such that EAB and EPQR are closely similar or identical.



Thus, when  $NAD^+$  binds a change in conformation permitting the subsequent binding of glutamate occurs.

Either at this point or when glutamate binds the proposed tightly bound metal ion would be exposed. In the absence of chelators, (or in their presence providing AMP or cations were present) the oxidative deamination reaction would take place. In the opposite direction - the reductive amination - the metal ion would be buried as previously proposed.

Thus, any molecular model must consider the 'microscopic reversibility' of the reaction with unidirectional inhibition. From the effector studies done one cannot but conclude that the reaction mechanism involves two distinct (at least in enzyme conformation) pathways for the two directions of the reaction. In the light of these studies the conclusion that gross conformation changes occur in the enzyme during the oxidative and reductive reactions may not be improbable. The extremely high levels of  $\text{NH}_4^+$  required in the reductive amination reaction make it attractive also to suggest that the apparent lack of control by multiple ligands in this reaction may be due to an alteration of the ionic state of the protein when  $\text{NH}_4^+$  is present.

## SECTION B. A Physiological Model of Mitochondrial Regulation

### I. Physiological Regulation of Glutamic Dehydrogenase

The NAD-specific glutamic dehydrogenase of Blastocladiella emersonii has been shown to be associated with the mitochondrion, presumably at the outer surface. This enzyme must play an important role in that it uniquely connects a large portion of amino acid and organic acid metabolism. It is not unrealistic to assume that complicated systems of control must have evolved to regulate its function, particularly because of its easy reversibility. Thus, the enzyme should be closely in tune with the energy producing and requiring processes of the mitochondria.

The adenylate control hypothesis of Atkinson (2), based on studies of phosphofructokinase and yeast NAD-specific isocitric dehydrogenase, predicted that AMP or ADP modulation would generally be found at branch points between biosynthetic and degradative pathways. On the basis of this hypothesis one may dissect the general problem of energy involvement in the control of metabolism at branch points by studying the modulating effects of adenylates (AMP, ADP, ATP) on the enzymes, individually and in combination

at these points. Glutamic dehydrogenase seems to fall into this category. Therefore, before developing an integrated system of mitochondrial regulation, it would seem advantageous to discuss glutamic dehydrogenase with the 'reversible' reaction it catalyses as an entity.

In order to illustrate the proposed regulation it is convenient to consider opposing metabolic conditions, i.e., "energized" as opposed to "unenergized" states of the mitochondria or high and low energy states. A representative scheme is outlined in Fig. 26.

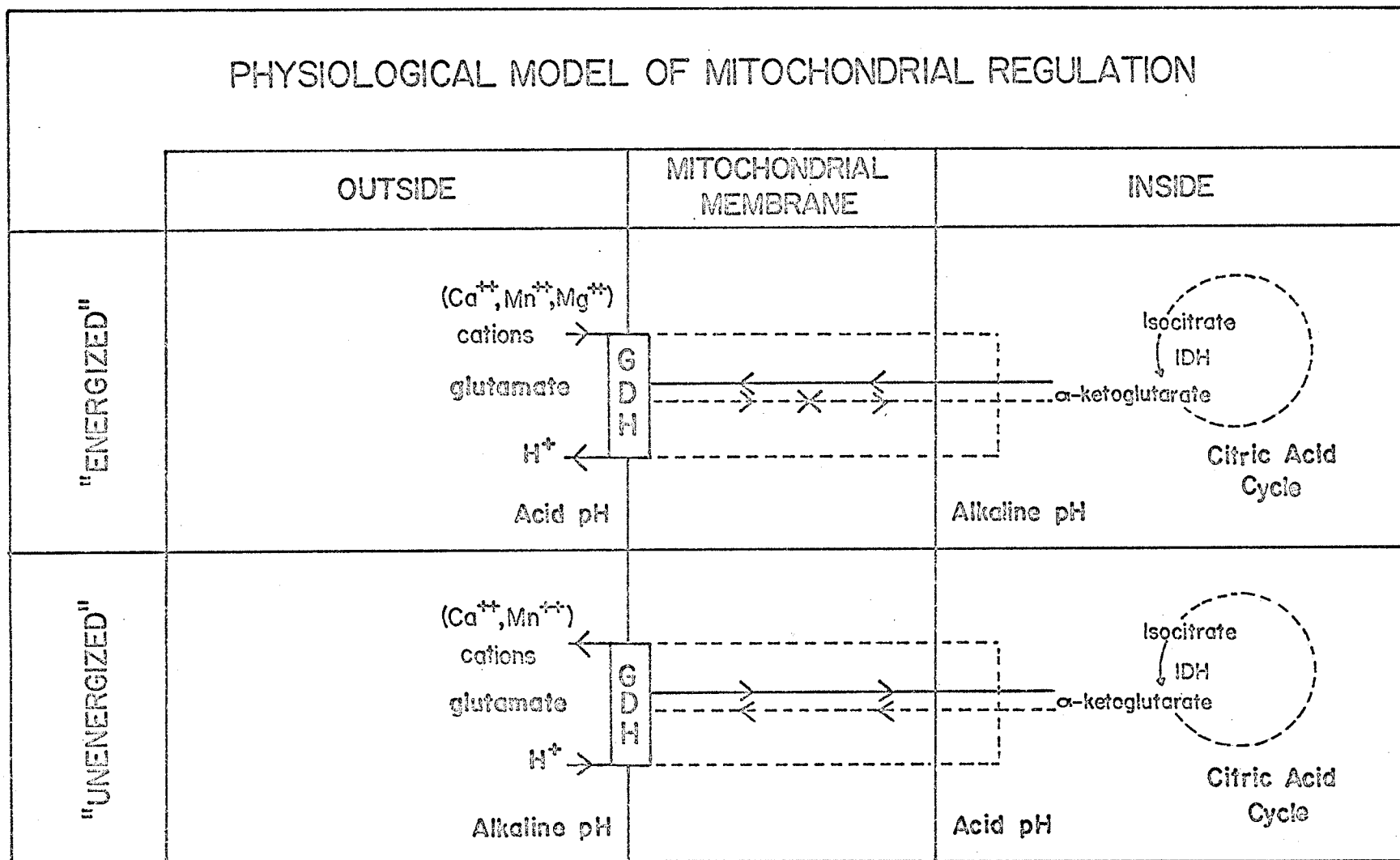
In the case of a high energy level within the cell cellular processes would be proceeding at a high rate. ATP would be readily available and the electron transport system can be considered as highly reduced due to the abundance of reducing power generated by the citric acid cycle. In such a state electronacceptors (oxygen) would be in relatively short supply. Considering the controls which must be operative, the cell must adapt to energy consuming processes if this excess energy is not to be wasted. The active uptake of ions into mitochondria is a well-documented energy requiring process. Partitioning of available energy between such energy requiring processes as ion transport and the storage of energy for future utilization must occur in order to utilize to the fullest

Figure 26. Physiological Model of Mitochondrial Regulation.

The implication of metabolic state and hence proton and cation fluxes on the activity of glutamic dehydrogenase and isocitric dehydrogenase from Blastocladiella.

X indicates reaction inhibited as described in text.

# PHYSIOLOGICAL MODEL OF MITOCHONDRIAL REGULATION



extent the energy made available. Considering these two processes (storage compound generation and ion translocation in the mitochondria) it may not be surprising if they involve closely integrated or even identical control systems.

It is well known that  $\text{Ca}^{++}$ ,  $\text{Sr}^{++}$ , and  $\text{Mn}^{++}$  may accumulate in mitochondria in the absence of an inducer (41).  $\text{Ca}^{++}$  uptake with simultaneous extrusion of protons is an energy-requiring process of mitochondria (26). This process may be supported by high energy intermediates generated via the electron transport system (26) or by a vectorially oriented, membrane bound ATPase (41). During ATP synthesis this ATPase effectively recombines hydroxyl ions and protons although separated by the mitochondrial membrane with consequent formation of ATP. During ATP hydrolysis protons are extruded from the mitochondria through a membrane generally impermeable to ions thereby establishing an electrochemical and/or pH gradient.

Localizing this general scheme to glutamic dehydrogenase one may now refer to the effect of  $\text{Ca}^{++}$  and  $\text{Mn}^{++}$  on the enzyme reaction.  $\text{Ca}^{++}$  was an activator of the reductive amination reaction, especially at low NADH levels. Conversely,  $\text{Ca}^{++}$  inhibited the oxidative deamination reaction, especially at low levels of glutamate. One can draw a tentative connection between  $\text{Ca}^{++}$  uptake and

generation of storage compounds via glutamate production. It is interesting to note that in the presence of impermeant anions and impermeant alkali cations (including ammonium ion in this category) or at high pH the ratio of  $\text{Ca}^{++}$  taken up to oxygen consumed may reach 'superstoichiometric' ratios (26). In the absence of permeant anions the ratio of  $\text{H}^+$  out to metal  $^{++}$  in is about one. With permeant anions present, however, this could be greatly reduced (26). The passage of protons out through the mitochondrial membrane would effectively lower the pH outside the mitochondria. If permeant anions are present, the extrusion of protons with the uptake of large amounts of  $\text{Ca}^{++}$  (and subsequent deposition of calcium salts) would tend to raise the intramitochondrial pH (26). Thus, the unidirectional inhibition of glutamate breakdown by various citric acid cycle intermediates and cations and the enhancement of the synthesis of glutamate under conditions described becomes understandable. At high glutamate levels  $\text{Ca}^{++}$  is able to relieve glutamate inhibition. This may be a complex control that regulates the level of glutamate present at any instant.

Before consideration is made of an "unenergized" state of the mitochondria, perhaps description of a transition would be apropos.

As energy is expended in the reactions described above, the ratio of AMP and ADP to ATP would increase. Also, excess citric acid cycle intermediates would be drained off to form storage compounds such as proteins, fats, glycogen. The uptake of  $\text{Ca}^{++}$  stimulates respiration and uncouples oxidative phosphorylation (26). The electron transport chain should become more oxidized. Studies have indicated that  $\text{Ca}^{++}$  activation of respiration and the oxidative phosphorylation of ADP involve the same energy-conserving points (26). Presumably the energy-requiring processes must slow down as the energy drain overtakes the source. In the specific case of glutamic dehydrogenase, as glutamate level rises, glutamate inhibition of glutamate breakdown is relieved by  $\text{Ca}^{++}$ . Together with a stimulation of respiration,  $\text{Ca}^{++}$  can provide the means for a compensatory effect on respiration creating a delicate balance between ATP synthesis and its breakdown.

One may further consider an "unenergized" state for the mitochondria. In such a state one must assume that an oxidizable substrate is not immediately available, hence a shortage of ATP. Thus,  $\text{Ca}^{++}$  can be extruded, not via diffusion along a concentration gradient, but rather by a process bearing characteristics of an enzyme controlled process (26). Protons would be taken up with resultant

relief of intramitochondrial alkalinization. Thus, uncoupling of oxidative phosphorylation by  $\text{Ca}^{++}$  may be relieved. Oxidations in the citric acid cycle would, however, proceed at a low level because of the lack of substrate. Thus, the inhibition of glutamate breakdown by intermediates would be relieved. As seen in AMP activation studies, increasing amounts of AMP shift the pH optimum for glutamate breakdown to a higher pH. Thus, the increased AMP plus ADP to ATP ratio and the extrusion of  $\text{Ca}^{++}$  ions could conceivably enhance glutamate breakdown. (Remember also that at high glutamate levels  $\text{Ca}^{++}$  would also stimulate glutamate oxidation into organic acids with the regeneration of ATP.)

By combining the two states one is able to derive a system by which momentary fluctuation in levels of energy metabolites could alternatively stimulate or inhibit one direction or the other of the enzyme reaction.

## II. Generalized Pattern of Mitochondrial Regulation

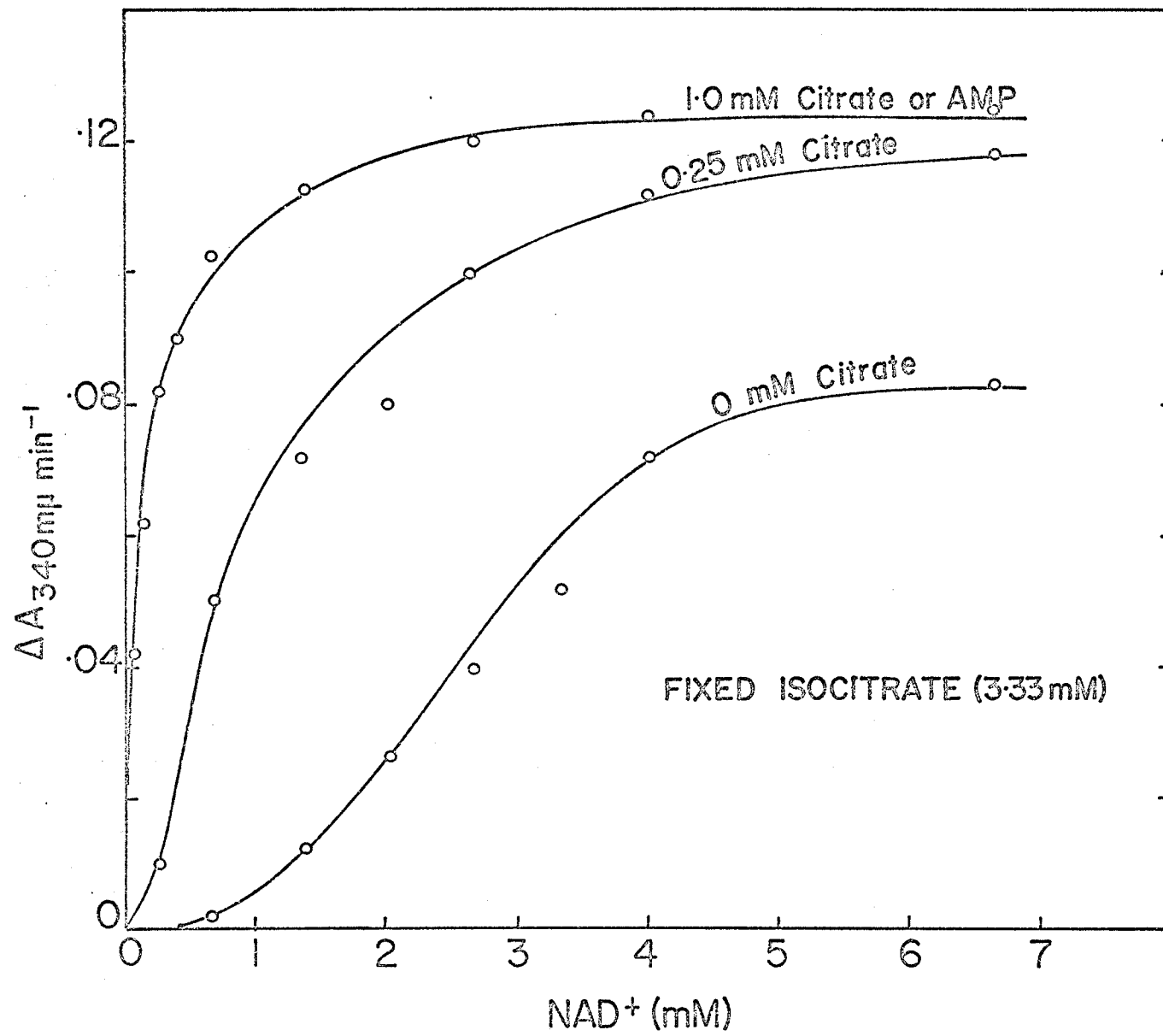
Keeping in mind the specific case of glutamic dehydrogenase, one may further extend this mitochondrial regulation to other enzymes of the citric acid cycle. Intensive study has been done with an NAD-specific isocitric dehydrogenase from Blastocladiella emersonii (39). This enzyme has also been found to be mitochondrial (39). If, as in other organisms, the NADP-specific enzyme is cytoplasmic

(35), these two enzymes would be effectively separated physically within the cell. The NAD-specific isocitric dehydrogenase has been found to be virtually irreversible and subject to regulation by compounds which also affect the glutamic dehydrogenase activity (39). In many instances, however, opposite controls converging on the  $\alpha$ -ketoglutarate locus seem operative. Studies seem to support the general pattern outlined in Fig. 26. The rate-concentration curves shown in Fig. 27 show that citrate, the strongest metabolite inhibitor of glutamate breakdown, is a very effective activator of isocitric dehydrogenase. The latter enzyme also exhibits a pH dependence of kinetic parameters such as modifier effects. The opposing effects of citrate on the two enzymes led to proposal of a regulatory mechanism.

In the "energized" state previously described citric acid cycle oxidations could proceed at a high rate. In this case isocitric dehydrogenase may be activated by the high citrate levels and the ready availability of  $Mn^{++}$  or  $Mg^{++}$  (as  $Mn^{++}$  is taken up by a method similar to  $Ca^{++}$ ). The reductive amination of  $\alpha$ -ketoglutarate is not inhibited, rather it is slightly activated by citrate AMP and ADP. Therefore, glutamate synthesis can proceed.

During the transition stage to a lower energy state, levels of citrate along with other citric acid cycle intermediates would drop and adenylate concentrations would change (AMP and ADP increasing in relation to ATP).

Figure 27. Rate of  $\text{NAD}^+$  reduction catalysed by an NAD-specific isocitric dehydrogenase from Blastocladiella against  $\text{NAD}^+$  concentration at different levels of citrate. Reaction mixtures contained 0.2 M Tris-acetate, pH 8; fixed isocitrate (3.33 mM); citrate as indicated.



Eventually an "unenergized" state would be reached. Cations would be extruded and protons taken up would effectively lower the intramitochondrial pH. As previously described inhibition of glutamate breakdown would be relieved. Simultaneously the extent of activation of the isocitric dehydrogenase by citrate and metal ions ( $Mn^{++}$ ,  $Mg^{++}$ ) would decline. However, AMP activation of the enzyme would continue thus ensuring cycling of citric acid cycle intermediates generated from glutamate toward ATP synthesis.

Thus, the steady-state condition of regulation would depend upon a delicate balance among the metabolites, adenylate concentrations, protons, and cations.

## REFERENCES

1. ATKINSON, D.E., Science (N.Y.), 150, 851, 1965.
2. ATKINSON, D.E., Annu. Rev. Biochem., 35, (1), 85, 1966.
3. ATKINSON, D.E., HATHAWAY, J.A., AND SMITH, E.C.,  
J. Biol. Chem., 240, 2682, 1965.
4. CANTINO, E.C., and HORENSTEIN, E.A., Mycologia,  
48, 777, 1956.
5. CANTINO, E.C., and LOVETT, J.S., Advance. Morphogenesis,  
3, 33, 1964.
6. CLELAND, W.W., Biochim. Biophys. Acta, 67, 104, 173, 188,  
1963.
7. CLELAND, W.W., Annu. Rev. Biochem., 36, (1), 77, 1967.
8. CORMAN, L., and KAPLAN, N.O., J. Biol. Chem., 242,  
2840, 1967.
9. FISHER, H.F., CROSS, D.G., and MCGREGOR, L.L., Nature  
(London), 196, 895, 1962.

10. FRIEDEN, C., Biochim. Biophys. Acta, 27, 431, 1958.
11. FRIEDEN, C., J. Biol. Chem., 234, 809, 1959.
12. FRIEDEN, C., J. Biol. Chem., 238, 3286, 1962.
13. FRIEDEN, C., J. Biol. Chem., 240, 2028, 1965.
14. FRIEDEN, C., and COLMAN, R.F., J. Biol. Chem., 242,  
1705, 1967.
15. FRIEDEN, C., J. Biol. Chem., 242, 4045, 1967.
16. GERHART, J.C., and PARDEE, A.B., J. Biol. Chem.,  
237, 891, 1962.
17. GOLDSTEIN, A., and CANTINO, E.C., J. Gen. Microbiol.,  
28, 689, 1962.
18. HALL, D.O., and GREENAWALT, J.W., J. Gen. Microbiol.,  
48, 419, 1967.
19. HATHAWAY, J.A., and ATKINSON, D.E., J. Biol. Chem.,  
238, 2875, 1963.

20. KING, E.L., and ALTMAN, C., J. Phys. Chem., 60, 1375, 1956.
21. KORMAN, K., in Molecular Insights into the Living Process, D.E. Green and R.F. Goldberger, Academic Press, N.Y., 1967, p. 121.
22. KOSHLAND, D.E., Science, 142, 1533, 1963.
23. KOSHLAND, D.E., Cold Spring Harbour Symp. Quant. Biol., 28, 473, 1963.
24. KOSHLAND, D.E., Fedn. Proc., 23, 719, 1964.
25. KOSHLAND, D.E., NÉMETHY, G., and FILMER, D., Biochemistry, 5, 365, 1966.
26. LEHNINGER, A.L., CARAFOLI, E., and ROSSE, C.S., Advance. Enzymol., 29, 259, 1967.
27. LEJOHN, H.B., Biochem. Biophys. Res. Commun., 28, 96, 1967.
28. LEJOHN, H.B., and McCREA, B.E., J. Bacteriol., 95, 87, 1968.

29. LEJOHN, H.B., SUZUKI, I., and WRIGHT, J.A., J. Biol. Chem., 243, 118, 1968.
30. LEJOHN, H.B., and JACKSON, S., J. Biol. Chem., 243, 3447, 1968.
31. LEJOHN, H.B., Biochem. Biophys. Res. Commun., 32, 278, 1968.
32. LEJOHN, H.B., J. Biol. Chem., 243, 5126, 1968.
33. LESSIE, P.E., and LOVETT, J.S., Amer. J. Bot., 55, 220, 1968.
34. LOVETT, J.S., and CANTINO, E.C., J. Gen. Microbiol. 24, 87, 1961.
35. LOWENSTEIN, J.M., in D.M. Greenberg, (Ed.), Metabolic Pathways, Vol. I., Ed. 3, Academic Press, N.Y., 1967, p. 147.
36. LOWRY, O.H., ROSEBROUGH, N.J., FARR, A.L., and RANDALL, R.J., J. Biol. Chem., 193, 265, 1951.

37. MAHLER, H.R., and CORDES, E.H., Biological Chemistry, Harper and Row, N.Y., 1966.
38. MARTIN, R.G., and AMES, B.N., J. Biol. Chem., 236, 1372, 1961.
39. McCREA, B.E., M.Sc. Thesis, University of Manitoba, 1969.
40. McCURDY, H.D., and CANTINO, E.C., Plant Physiol., 35, 463, 1960.
41. MITCHELL, P., Advance. Enzymol., 29, 33, 1967.
42. MONOD, J., CHANGEUX, J.P., and JACOB, F., J. Mol. Biol., 6, 306, 1963.
43. MONOD, J., WYMAN, J., and CHANGEUX, J.P., J. Mol. Biol., 12, 88, 1965.
44. OLSEN, J.A., and ANFINSON, C.B., J. Biol. Chem., 197, 67, 1952.
45. PASSONNEAU, J.V., and LOWRY, O.H., Biochem. Biophys. Res. Commun., 7, 10, 1962.

46. PASSONNEAU, J.V., in G. WEBER, (Ed.), Advance. in Enzyme Regulation, MacMillan, N.Y., 1964, p. 265.
47. PULLMAN, M.E., and SCHATZ, G., Annu. Rev. Biochem., 36, 539, 1967.
48. RASMUSSEN, H., CHANCE, B., and OGATA, E., Proc. Nat. Acad. Sci. U.S., 53, 1069, 1965.
49. REINER, J.M., in The Organism as an Adaptive Control System, Prentice Hall, N.Y., 1968.
50. SANWAL, B.D., STACHOW, C.S., and COOK, R.A., Biochemistry, 4, 410, 1965.
51. SANWAL, B.D., and COOK, R.A., Biochemistry, 5, 886, 1966.
52. STACHOW, C.S., and SANWAL, B.D., Biochem. Biophys. Res. Commun., 17, 318, 1964.
53. TOMPKINS, G.M., and YIELDING, K.L., Cold Spring Harbour Symp. Quant. Biol., 26, 331, 1961.

54. TOMPKINS, G.M., YIELDING, K.L., and CURRAN, J.F.,  
Proc. Nat. Acad. Sci. U.S., 47, 270, 1961.
55. TOMPKINS, G.M., YIELDING, K.L., TALAL, N., and  
CURRAN, J.F., Cold Spring Harbour Symp. Quant.  
Biol., 28, 461, 1963.
56. UMBARGER, H.E., J. Biol. Chem., 233, 415, 1958.
57. VAGELOS, P.R., ALBERTS, A.W., and MARTIN, D.B.,  
J. Biol. Chem., 238, 533, 1963.
58. WYMAN, J., Cold Spring Harbour Symp. Quant. Biol.,  
28, 483, 1963.